Basin Research

EAGE

Basin Research (2010) doi: 10.1111/j.1365-2117.2010.00497.x

Timing and mechanisms controlling evaporite diapirism on Ellef Ringnes Island, Canadian Arctic Archipelago

Jennifer Boutelier,* Alexander Cruden,*[1] Tom Brent† and Randell Stephenson‡

*Department of Geology, University of Toronto, Toronto, ON, Canada
†Geological Survey of Canada, Calgary, AB, Canada
‡Geology and Petroleum Geology, School of Geosciences, University of Aberdeen, Aberdeen, Scotland

ABSTRACT

The Permo-Carboniferous to Eocene Sverdrup Basin in Canada's Arctic Archipelago is strongly influenced by evaporite diapirism. However, salt structures within the basin have not been extensively investigated recently due to their remote location. This study includes the interpretation of legacy seismic reflection and borehole data to characterize the geometry of selected evaporite domes, and 1D backstripping of wells to investigate tectonic and sedimentary influences on diapirism. Extensional rift-structures appear to have played a significant role in the formation of evaporite domes by triggering and directing salt movement. Diapirism was initiated by at least the Middle Triassic and continued to develop during the Mesozoic. Differential loading of salt on opposing east–west dome margins led to their present day asymmetric geometries. Diapir growth rates in the Mesozoic were closely linked to the rate of sedimentation and influenced by regional tectonism.

INTRODUCTION

Ellef Ringnes Island is located within the Sverdrup Basin, a pericratonic trough that formed along a northeast–southwest-oriented continental rift zone located in the Canadian Arctic Archipelago (Fig. 1). The steep-sided basin is estimated to contain up to 13 km of Carboniferous to Eocene strata at the basin axis (Balkwill, 1978). The Carboniferous Otto Fiord Formation is composed of the initial evaporitic (gypsum, anhydrite and halite) transgressive fill of the basin (Davies & Nassichuk, 1991). At the basin margins, complete exposed sections of the Otto Fiord Formation predominantly consist of anhydrite interlayered with limestone and reach up to 400 m in thickness (Davies & Nassichuk, 1975).

Mobilization of salt from the Otto Fiord Formation has led to the formation of approximately 100 piercement structures in the basin centre, the majority of which are located on Axel Heiberg and the Ringnes islands (Fig. 1; Thorsteinsson, 1974). Evaporite structures range from large concentric evaporite stocks in the western region to linear or crooked evaporite walls separated by broad synclinal basins in the eastern region of the basin.

With the exception of studies of salt canopies on Axel Heiberg Island (Jackson & Harrison, 2006; Harrison & Jackson, 2008) and the salt-based fold belt on Melville Island (Harrison, 1995), little recent research and exploration has been completed on the timing and mechanisms controlling the initiation and mobilization of salt structures in the Sverdrup Basin. This study investigates the evolution of evaporite piercement structures on Ellef Ringnes Island with particular focus on the Dumbells, Contour and Hoodoo domes (Fig. 2). To better understand the mechanisms controlling the formation of these structures, an analysis of legacy seismic reflection and borehole data was completed to constrain the 3D geometry of the domes. In addition, 1D backstripping analysis was undertaken in an attempt to identify possible tectonic triggers and periods of subsidence modified by diapirism in wells adjacent to evaporite piercement structures.

Correspondence: Jennifer Boutelier, University of Toronto, Toronto, ON, Canada. E-mail: macauley.jenny@gmail.com
[1]Present address: School of Geosciences, Monash University, Melbourne, Victoria, Australia.

TECTONIC SETTING

The first initial rifting phase of the Sverdrup Basin occurred from the early Carboniferous to early Permian with an initial basin fill that consists of nonmarine conglomerates and sandstones overlain by a progressive sequence of evaporite to deep water deposits that formed as subsidence exceeded deposition (Davies & Nassichuk, 1991). Active rifting of the basin ended in the Middle to Late Permian and was followed by a period of passive post-rift crustal subsidence driven by thermal contraction and sediment loading (Stephenson *et al.*, 1994). By the end of the Palaeozoic, a deep basin had formed with an estimated bathymetric difference of 2 km or more between the basin margin and centre (Embry & Beauchamp, 2008).

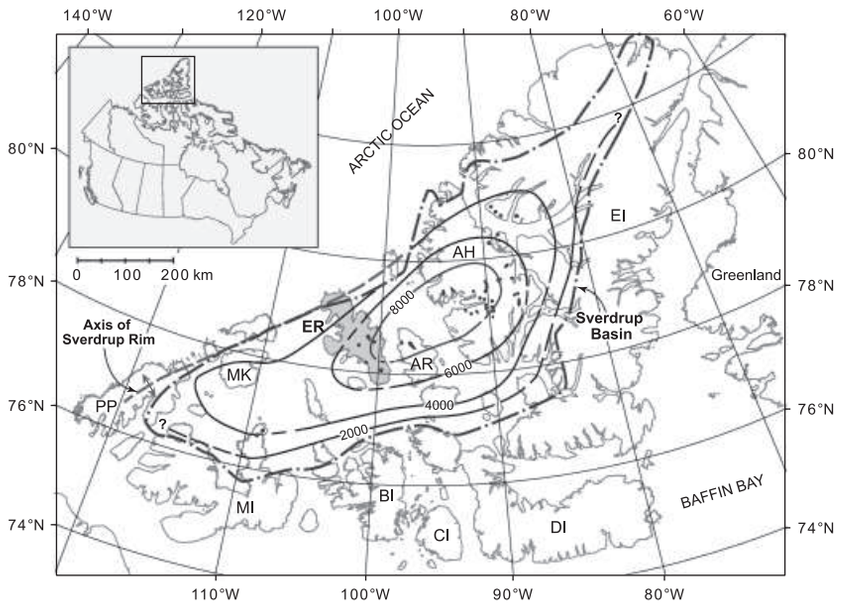

Fig. 1. Sverdrup Basin, Canadian Arctic Archipelago. Map inset shows the location of the basin with respect to Canada. Key: AH, Axel Heiberg Island; AR, Amund Ringnes Island; BI, Bathurst Island; CI, Cornwallis Island; DI, Devon Island; EI, Ellesmere Island; ER, Ellef Ringnes Island (shaded grey); MI, Melville Island; MK, Mackenzie King Island; and PP, Prince Patrick Island. The approximate limits of the basin and the Sverdrup rim are indicated by stippled and dashed lines, respectively. Regional scale onshore salt structures are included as black dots. Isopach contours of Mesozoic strata (in meters) are also included (taken from Embry, 1991).

The basin evolved rapidly in the Triassic with continual filling by thick deposits of siltstones and shales (Embry, 1991; Embry & Beauchamp, 2008). By the end of the Norian, the central portion of the basin had been completely filled, replacing the previously deep water centre with a shallow seaway.

Rift activity related to the initiation of the Amerasia Basin to the northeast began to notably affect the Sverdrup Basin in the Middle Jurassic. This led to the formation and uplift of a narrow strip of land, referred to as the Sverdrup Rim, that separated the Sverdrup Basin from the developing Amerasian Basin (Fig. 1; Embry & Beauchamp, 2008). Post-rifting thermal subsidence in the Mesozoic was further interrupted in the early Cretaceous (latest Valanginian–earliest Hauterivian) by regional uplift interpreted to coincide with the initiation of seafloor spreading and creation of oceanic crust in the adjacent Amerasian Basin (Embry & Dixon, 1994). Renewed rifting and extension followed the early Cretaceous uplift event and is characterized by increased subsidence and sediment supply rates, normal faulting and magmatism (Balkwill, 1978; Embry & Osadetz, 1988; Embry, 1991; Stephenson *et al.*, 1994; Villeneuve & Williamson, 2006).

In its final stage of development, the Sverdrup Basin was tectonically modified and inverted during the Palaeogene Eurekan orogeny due to the collision between Greenland and Ellesmere Island (Balkwill, 1978; Miall, 1984). The resulting build-up of compressional stresses led to large-scale lithospheric failure in the Middle Eocene, producing several basin highs (Stephenson *et al.*, 1990; Oakey & Stephenson, 2008) that restricted sedimentation within intermontane sedimentary basins (Miall, 1991; Ricketts & Stephenson, 1994). The Eurekan orogeny is also responsible for further uplift and erosion of the Sverdrup Rim and the development of a fold-and-thrust belt on Ellesmere and eastern Axel Heiberg islands.

GEOLOGY OF THE STUDY AREA: ELLEF RINGNES ISLAND

Ellef Ringnes Island extends from the Sverdrup Rim in the north to the basin axis in the south. The central and southern regions of the island consist of conformable successions of Mesozoic formations with the youngest units confined to the axes of regional northwest–southeast-oriented synclines (Stott, 1969). The northern Isachsen Peninsula is composed of Neogene deposits that rest unconformably on uplifted and eroded Late Triassic to Late Jurassic Sverdrup Basin rocks.

At depth, the study area is underlain by a succession of Late Palaeozoic to Early Mesozoic carbonate and deep marine/prodelta siltstones and shales (Fig. 3; Davies & Nassichuk, 1991; Embry, 1991). These marine deposits are overlain by the Late Triassic to Early Jurassic Heiberg Formation, consisting of delta front shales, siltstones and sandstones grading to coarser delta plain and shallow marine shelf deposits. Beneath the western regions of the island, the Heiberg Group is split into five formations, three sandstone dominant units separated by two shale-siltstone dominant units representing the intercalation of thin beach to marine shelf sandstones and prodelta/shelf muds and silts. The Heiberg Formation is overlain by shale and siltstone shelf deposits of the Jameson Bay, McConnell Island, Ringnes and Deer Bay formations, punctuated by thin marine and deltaic sandstone deposits of the Awingak and Sandy Point formations. The Early Cretaceous Isachsen Formation, dominated by medium to coarse-grained delta plain and fluvial channel deposits, lies unconformably on the Deer Bay Formation at the basin margins. Thick conformable Cretaceous formations (Christopher, Hassel and Kanguk) alternate between siltstone and sandstone dominant units of marine shelf, shoreline and shallow shelf origin. The Kanguk Formation is capped by shoreline to shallow marine

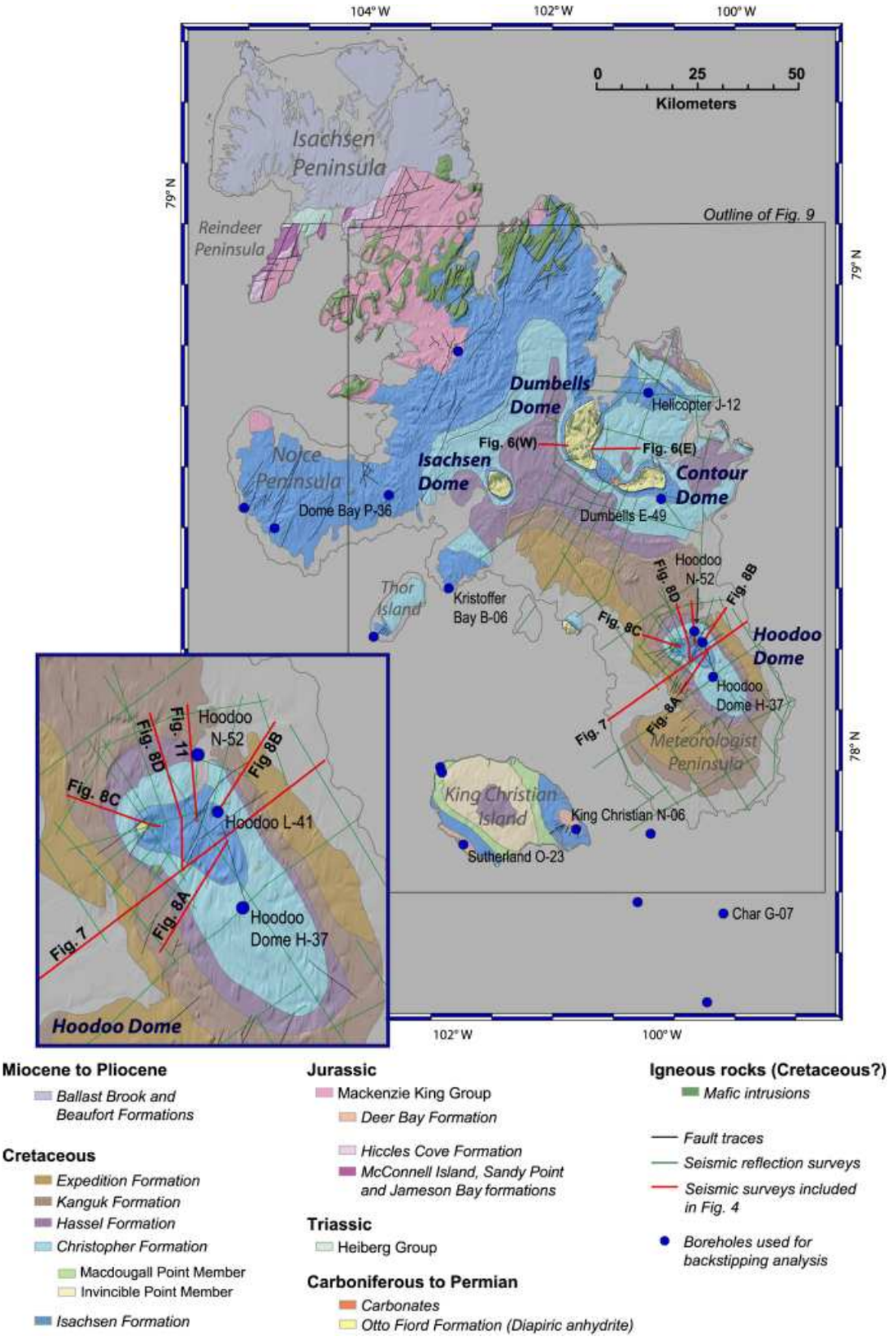

Fig. 2. Map of Ellef Ringnes Island with labelled evaporite piercement structures. The bedrock geology is the unpublished compilation work of C. Harrison. The maps used in the compilation include Stott (1969) for Ellef Ringnes Island and Balkwill & Roy (1978) for King Christian Island. The orientation and distribution of all seismic reflection surveys interpreted in this study are outlined in green and highlighted in red for surveys included in Figs 6–8. Locations of boreholes used for backstripping are included in blue and labelled for wells included in Fig. 12. A magnified view of Hoodoo Dome is included in the map inset.

sandstones and unconsolidated sands (Expedition Formation) that prograded into the basin during the Late Cretaceous (Stott, 1969; Embry & Beauchamp, 2008).

The surface and subsurface of Ellef Ringnes Island contains an abundance of mafic intrusions that occur in the form of dykes and sills mostly concentrated within Jurassic and Early Cretaceous formations and as relatively unaltered blocks within evaporite piercement structures. The erosional pattern of saucer-shaped sills produces circular to elliptical outcrop patterns in the southern region of Isachsen Peninsula within the Mackenzie Group (undifferentiated Ringnes and Deer Bay Formations; Fig. 2). Larochelle & Black (1963) estimated the age of the intrusions to be between 102 and 110 Ma, correlating with the average ages of the Sverdrup Basin Magmatic Province (Villeneuve & Williamson, 2006). The blocks entrained within the piercement structures have not been dated, but are also suspected to be of Cretaceous age (Stott, 1969).

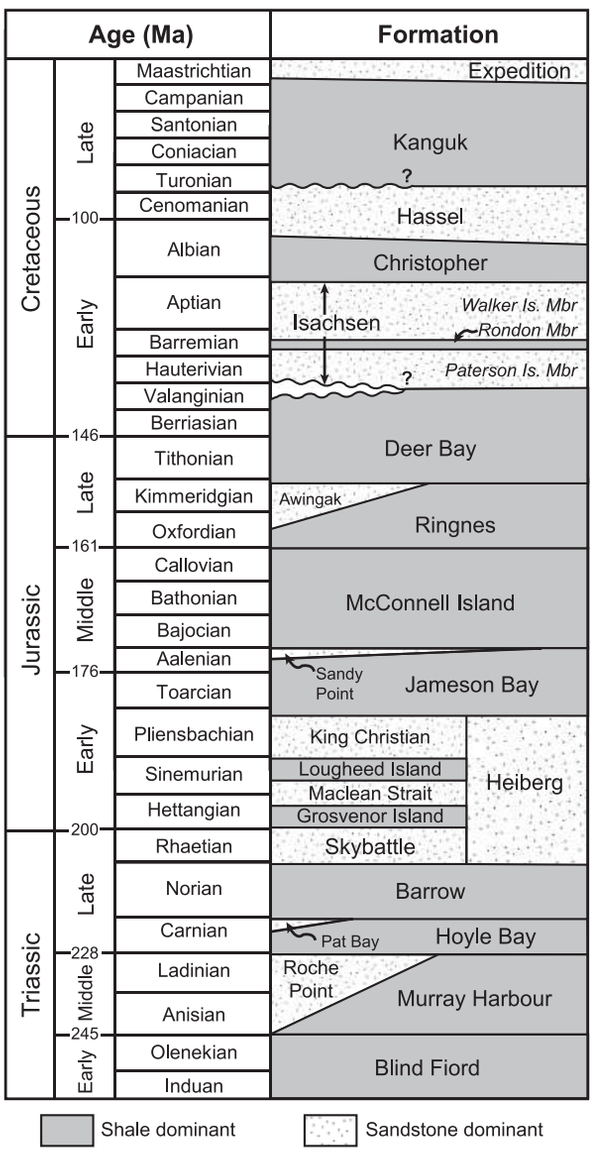

Fig. 3. Mesozoic stratigraphy of Ellef Ringnes Island (derived from Embry, 1991; Dewing & Embry, 2007).

DESCRIPTION AND EVOLUTION OF SALT STRUCTURES WITHIN THE SVERDRUP BASIN

Large, concentric diapirs are most common in the western region of the Sverdrup Basin on the Ringnes islands, Sabine Peninsula (Melville Island) and western Axel Heiberg Island. Except for a few cases where salt is exposed (e.g. Hugon & Schwerdtner, 1982), the domes at surface are composed of gypsified anhydrite caps covering halite cores. From their first discovery, the anhydrite caps were recognized to be of primary sedimentary origin and were most likely mobilized together with the underlying salt (Heywood, 1955). The caps are estimated to range from 200 to 800 m in thickness from measured sections and gravity studies (Schwerdtner & Clark, 1967; Spector & Hornal, 1970; Davies & Nassichuk, 1975).

On Ellef Ringnes Island, ovate evaporite structures are aligned within regional anticlines and are in contact with the Isachsen Formation at surface. Dumbells, Contour and Isachsen Domes are exposed at surface whereas Hoodoo Dome is buried under a thin cover of the Isachsen Formation. Along the Dumbells Dome contact, the Isachsen Formation dips steeply away from the dome with orientations of up to 80° (Fig. 4a; Stott, 1969; Van Leeuwen, 2005). The anhydrite caps are relatively unaltered in the centre of the dome with highly sheared margins (Fig. 4b; Heywood, 1955; Van Leeuwen, 2005).

In the central and eastern regions of Axel Heiberg Island, the style of salt structures differs with the occurrence

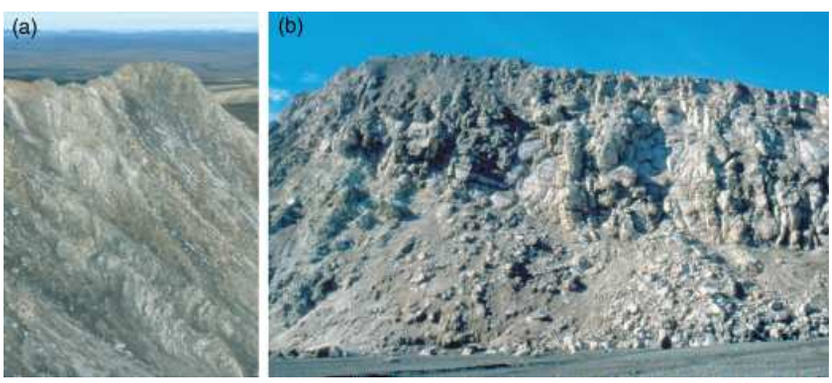

Fig. 4. Photographs of Dumbells Dome, illustrating the (a) steeply inclined and sheared anhydrite-dominant marginal phase, view looking north, southeast dome margin and (b) gently folded subhorizontal primary bedding in anhydrite-dominant cap, view looking west, south centre of dome.

of linear to crooked walls separated by broad synclinal basins, known as the 'wall-and-basin' structure (or WABS) region (Thorsteinsson, 1974; van Berkel *et al*., 1984). The development of diapirs and salt structures on Axel Heiberg Island was originally believed to be related to the Palaeogene Eurekan orogeny (Thorsteinsson & Tozer, 1960; Fortier *et al*., 1963). However, subsequent studies suggest that the Eurekan event merely overprinted pre-existing structures, deforming them into the tight anticlinal folds of the WABS region (van Berkel *et al*., 1984; Jackson & Harrison, 2006). Stratigraphic evidence adjacent to diapirs unaffected by orogenic shortening (i.e. western regions of the basin) confirm that the majority of structures experienced a long period of growth dating back to at least the early Mesozoic (e.g. Gould & DeMille, 1964; Hoen, 1964; Stott, 1969; Schwerdtner & Osadetz, 1983; van Berkel *et al*., 1984; van Berkel, 1989). Common mechanisms proposed for the initiation and localization of diapirism includes differential loading from thick prograding deposits (Gould & DeMille, 1964; Balkwill, 1978; Jackson & Harrison, 2006), differential loading on top of faulted basement blocks (Schwerdtner & Osadetz, 1983; Stephenson *et al*., 1992), and reactive diapirism triggered by rift-related extension (Jackson & Harrison, 2006).

SEISMIC REFLECTION PROFILES

This study focuses on the interpretation of a subset of legacy industry 2D seismic reflection data originally acquired by multiple companies from 1969 to 1973 (Figs 5–8). Interpreted seismic lines were chosen to encompass the central and southern regions of Ellef Ringnes Island with detailed coverage of Hoodoo, Dumbells and Contour domes (Fig. 2). Seismic reflection surveys are restricted to 2D single to sixfold post-stacked data with varying quality of resolution. The majority of lines analyzed in this study were filtered and geographically corrected. Many of the lines approaching Dumbells, Contour and Hoodoo Dome were also migrated using the Kirchoff method. A visual comparison of migrated and unmigrated seismic reflection data is provided in Fig. 5.

Seismic interpretation

Formation boundaries picked as horizons within seismic profiles were interpreted based on the picked tops from wells within the central and southern regions of the island (Dewing & Embry, 2007). The majority of wells located within this region were drilled to the top of the main oil and gas hosting reservoir rock, the porous sandstone-dominant King Christian Formation and correlative upper portion of the Heiberg Formation. Control on formation tops therefore dates as far back as the Late Triassic–Early Jurassic. Owing to these stratigraphic constraints, the study focuses primarily on the development of the domes during the Mesozoic. Depth intervals were converted to time using velocity–time pairs from check shot surveys to allow for comparison and overlay of well logs on intersecting seismic profiles. Picked horizons were analyzed alongside synthetic well logs produced for the above boreholes. Lines that do not intersect wells were tied in with neighbouring and cross-cutting seismic surveys. The Christopher and younger formation horizons are not intersected by any wells and were therefore approximated from surface outcrops (Stott, 1969).

Limitations in the interpretation of horizons are mostly due to the low quality and resolution of the data, which often smears out detailed structures such as faults and unconformities. This is most problematic in imaging near-surface faults related to salt movement. In addition, highly reflective permafrost layers and mafic sills (reaching thicknesses of up to 140 m) mask underlying horizons. Interpretation of evaporite bodies is complicated around Hoodoo Dome, where salt overhangs or wings diminish the signal of underlying sedimentary units as most of the seismic energy is reflected at the salt boundary. Steeply

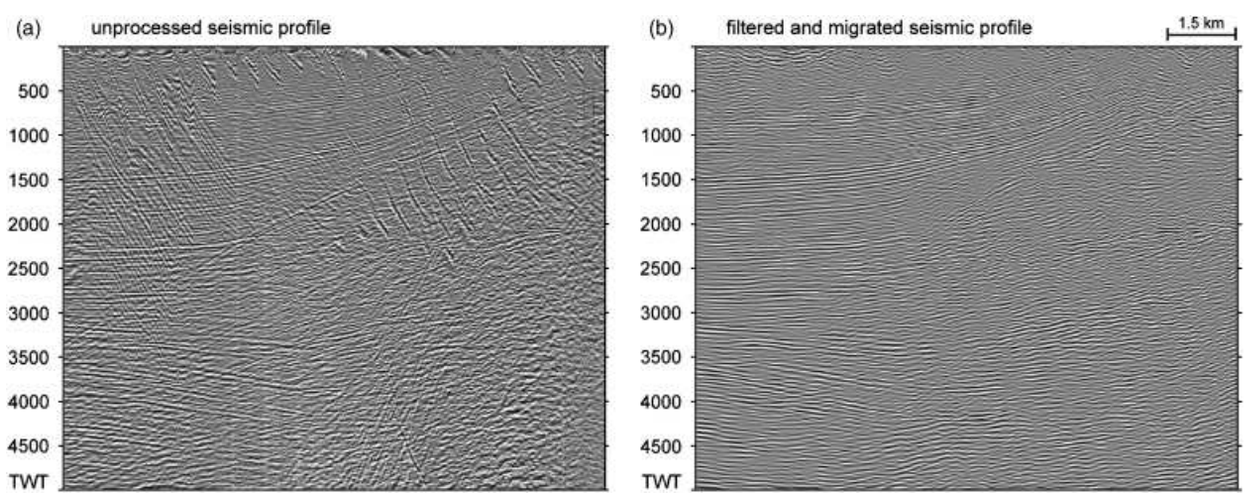

Fig. 5. Comparison of unmigrated and unfiltered seismic profile (Fig. 8d) with the migrated and filtered version. Location of profile is included in Fig. 2. The seismic profile is the property of Imperial Oil Resources.

dipping dome margins and adjacent drape-folded formations also proved to be difficult to interpret.

For some profiles (e.g. Fig. 7), gravity was recorded in conjunction with seismic acquisition and aids in the interpretation of evaporite boundaries; however, the Bouguer anomaly data are of low spatial resolution making it difficult to define residual anomalies associated with the presence of salt or deeper crustal structures.

Depth conversion and isochore maps

To identify regional thinning/thickening trends across central and southern Ellef Ringnes Island, depth conversion of interpreted seismic horizons was conducted to produce isochore maps of each formation (Fig. 9). For consistent ties between all of the seismic surveys, only interpreted horizons of un-migrated data were used. Composite velocity (sonic) logs derived from multiple wells were produced for each formation in an attempt to capture velocity profiles over the largest range of depths. To characterize the general trend in velocity with depth, curves were fit to the composite sonic plots (e.g. Fig. 10). For multilayer time–depth conversion, the travel path of the seismic wave through overlying layers needs to be considered; therefore a layer-cake depth conversion was completed. To estimate interval velocities required for depth conversion of each layer in two-way travel time, 'instantaneous' velocities from sonic logs were integrated to give linear and power law approximations for the velocity variation with depth (Hillis *et al.*, 1995; Al-Chalabi, 1997). Power law functions were applied to the oldest formations as they better reflect the change in the velocity rates with depth due to compaction (e.g. Fig. 10).

Isochore maps presented in Fig. 9 are consistent with observations in boreholes ($\pm$ 50 m). The largest deviation from known thicknesses occurs in the northeastern region where seismically determined thicknesses are underestimated for the Ringnes Formation by 100–150 m. This error is most likely due to the occurrence of thick mafic sills in this region as the higher velocities of the sills are not accounted for in the depth conversion.

Main results

Dome asymmetry

Interpreted east–west oriented seismic profiles across Dumbells and Hoodoo domes reveal asymmetric geometries within adjacent sedimentary units (Figs 6 and 7). Both profiles share similar characteristics with generally thicker sedimentary packages occurring at deeper structural levels on the eastern margins of the domes. This is supported by isochore maps, which show thicker packages of sediments east of Dumbells Dome and east–northeast of Hoodoo Dome (more prominent in the Late Jurassic to Cretaceous formations). For Dumbells Dome, this thickness variation is also accompanied by the occurrence of a shallow rim syncline located approximately 5 km from the edge of the piercement structure (Fig. 6). The spatial extent of this rim syncline is confined within the concave curvature of Dumbells and Contour domes, as is seen in the isochore maps of the Deer Bay and Isachsen formations (Fig. 9d and e).

The structural offset on the eastern side of Dumbells Dome is accommodated by thinning of rotated or draped beds toward the dome margin. At Hoodoo Dome, the noticeable structural offset of formations is partially accommodated by a near vertical fault or shear zone where the coherency of the stratal reflections is lost on the seismic section. The eastern fault block is offset downward and can be traced through multiple east–west oriented seismic sections, giving a fault trace that is parallel to the axial trace of the Hoodoo Dome anticline. The effects of this zone can be seen at surface as apparent narrowing of the Hassel and Kanguk formations. The shear zone is also detected as a slight perturbation of the Bouguer gravity profile (Fig. 7).

In addition to thicker units on the eastern side of Hoodoo Dome, a consistent pattern of 'diverging' seismic reflections exists along the north–northeast margin (e.g. Fig. 8d). The

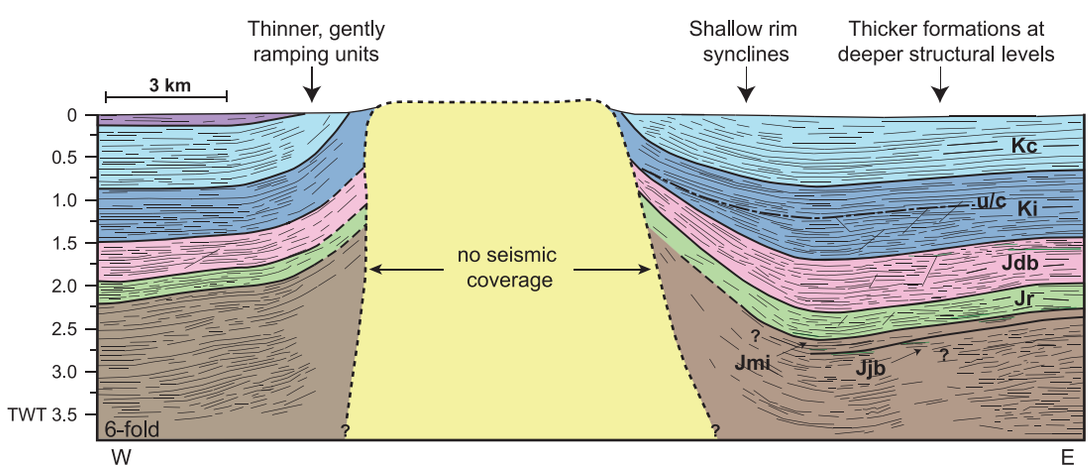

Fig. 6. Line drawing of seismic profiles illustrating the asymmetry of Dumbells Dome (location on Fig. 2). Seismic profiles are migrated with a vertical exaggeration of ~1.5. Key for formations is included in Fig. 7.

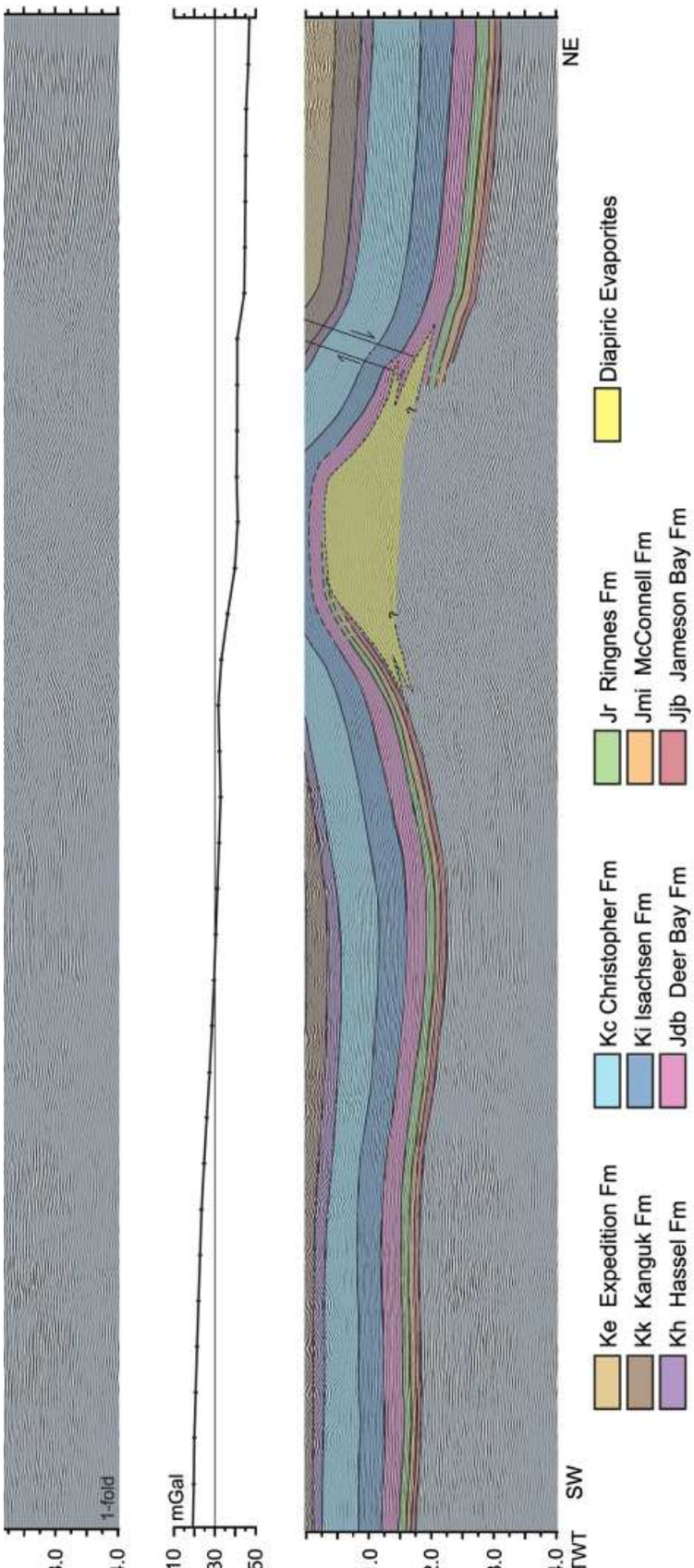

Fig. 7. Migrated seismic profile and corresponding Bouguer gravity signature illustrating the southwest–northeast asymmetry of Hoodoo Dome (location on Fig. 2). Seismic profile is onefold data with both interpreted and uninterpreted versions. The seismic profile was originally acquired by Panarctic Oils Ltd. and is currently owned by Suncor Energy Inc.

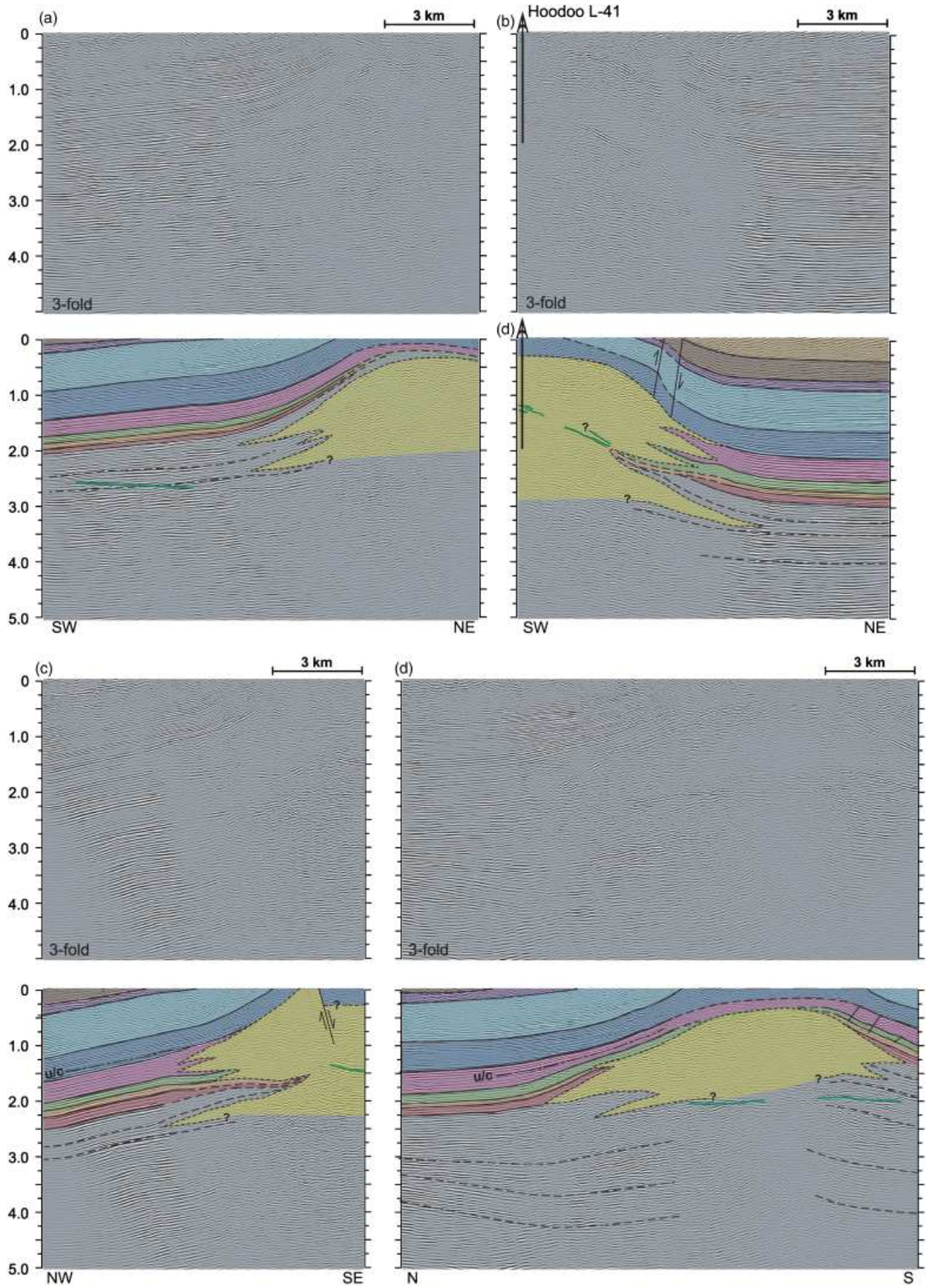

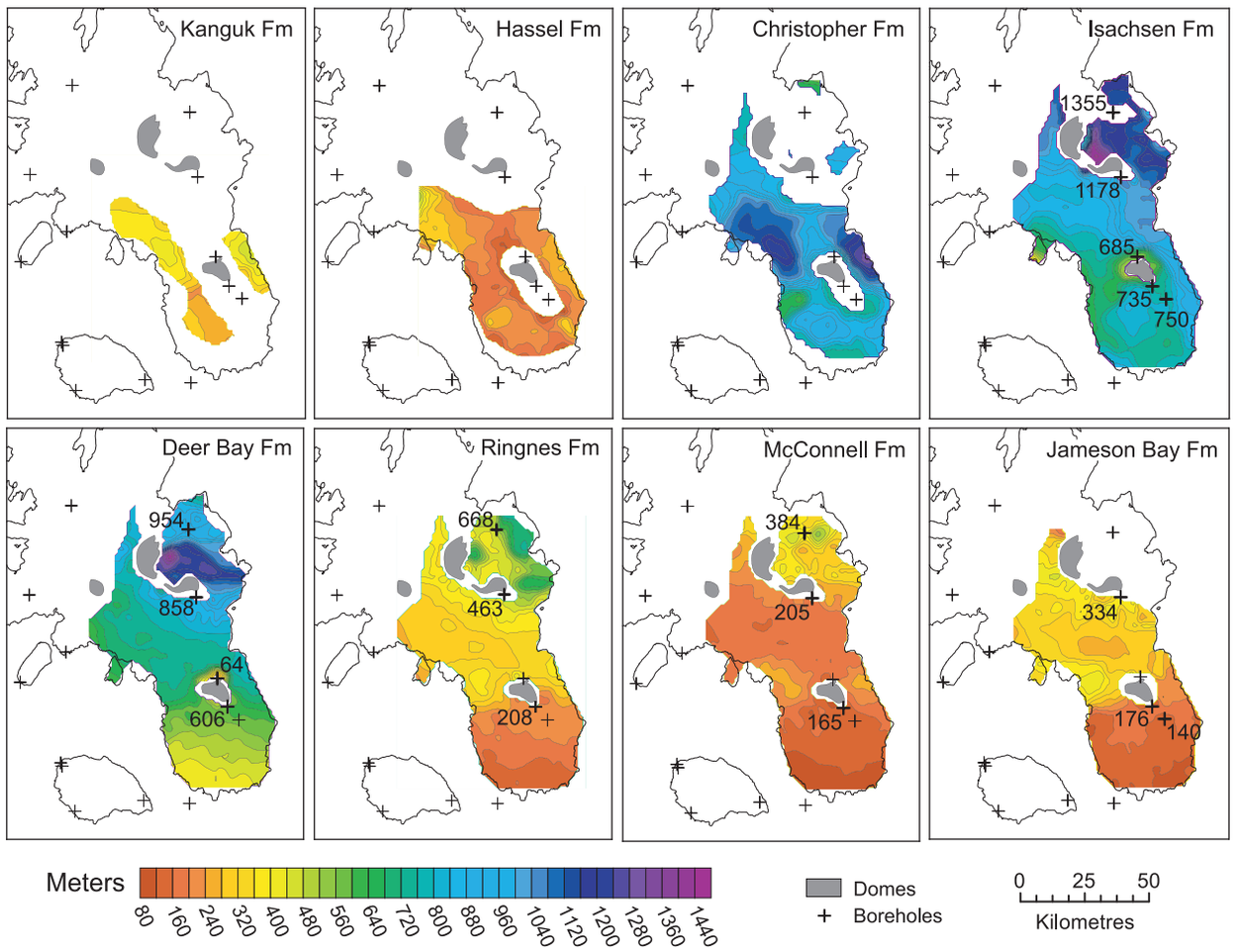

Fig. 9. Isochore maps derived from the depth conversion of seismic horizons. The colour scale represents the thickness of each formation. Vertical formation thicknesses (in meters) from boreholes are included on individual diagrams. The general location and geometry of piercement structures are highlighted in grey. Location of map inset included in Fig. 2.

reflections within adjacent sedimentary units diverge approaching the dome margins, with units dipping downward beneath the interpreted top of the Heiberg Formation. With migration, these features collapse into broad open synclines that appear to extend beneath interpreted salt wings (described in the following section). This divergence may have produced thickening of the Ringnes, McConnell Island and Jameson Bay formations along the north–northeast margin of Hoodoo Dome (Fig. 9f–h), however, the variation in thickness is less pronounced for these formations and may instead be a product of poor precision of picked horizons at structurally deeper levels.

Salt wings/debris flows at Hoodoo Dome

Little evidence is present in seismic lines to suggest that any salt bodies radiate away from Dumbells and Contour domes beneath adjacent sedimentary sequences. The partial sedimentary cover of Hoodoo Dome, however, allows for better coverage of seismic reflection data on the top of the dome (Fig. 2). Strong reflections in some seismic profiles mark the transition from low velocity overlying sediments to contrasting higher velocities of anhydrite and halite at the crest of Hoodoo Dome (e.g. Fig. 8c). The evaporite margins, however, are typically difficult to identify, leading to the notion of irregular and complex evaporite dome boundaries, such as 'Christmas tree' geometries. The tips of multiple flanges are interpreted as salt wings or overhangs in migrated profiles (Figs 7 and 8) that protrude from the main diapir stock. The presence of higher velocity horizontal salt bodies within adjacent syn-sedimentary units may explain why the coherency of horizons beneath these structures often degrades significantly at depth. Alternatively, some or all of the interpreted salt

Fig. 8. Select migrated seismic profiles with and without interpretations for Hoodoo Dome (locations in Fig. 2). All seismic profiles are threefold data. Some horizons beneath the top of the Heiberg Formation are also included as dashed lines to highlight the occurrence of salt wings, diverging sedimentation, etc. Interpreted mafic sills and dykes are highlighted in green. Seismic profiles are the property of Imperial Oil Resources.

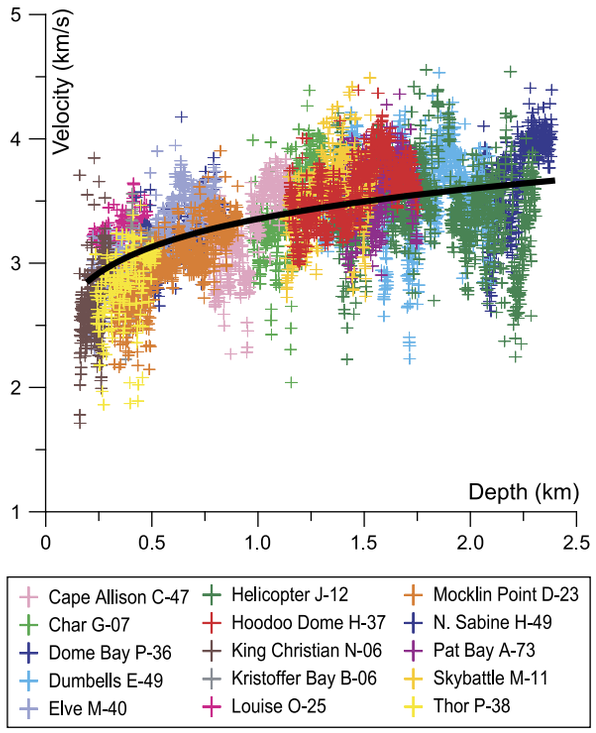

Fig. 10. 'Instantaneous' velocity with depth signature of the Deer Bay Formation derived from a compilation of sonic logs from multiple wells (see legend). The best fit power law curve (black) is $v_z = (1677\ \mathrm{m\ s^{-1}})\, z^{0.100}$ where v_z is the instantaneous velocity and z is depth. This formula is integrated over the seismic time range to approximate the interval velocity of the formation.

wings could represent debris flows that were shed off the flanks of rising diapirs when steep unstable slopes were generated by diapiric inflation at the surface (Giles & Lawton, 2002). Debris flows have been previously reported in the Sverdrup Basin adjacent to Axel Heiberg Island diapirs within early Cretaceous sediments onlapping salt canopies (Jackson & Harrison, 2006).

The number and extent of flanges surrounding Hoodoo Dome are complex and highly variable between neighbouring seismic lines. On the southwest margin of the dome, interpreted salt wings or debris flows extend within or beneath the Heiberg Formation, constraining the age of the oldest interpreted flanges to be at least Late Triassic (Fig. 8a). Further north, the number and complexity of flanges increase, suggesting smaller, higher frequency salt wings or debris flows (e.g. Fig. 8c). The interpretation of thinner, higher frequency flanges is open for debate; however, the first order signatures are convincing. Along the east–northeast boundary of Hoodoo Dome, the number and complexity of flanges increase even further, with the youngest interpreted salt wing/debris flow occurring at the top of the Deer Bay Formation (Fig. 8b).

Deformation in adjacent overburden

On the dome margins, formations are thinned and rotated upward (i.e. drape folded) during syn-halokinetic sedimentation. Thinning is most evident during the Late Jurassic and Early Cretaceous within the Deer Bay and Ringnes formations. Early to Middle Jurassic formations are most likely thinned and rotated upward as well; however, the image quality of these units degrades with depth and in areas with overlying salt wings. Isachsen and younger formations display the least thinning along dome margins. Thinning adjacent to the eastern margin of Dumbells Dome is quite dramatic. Here, the vertical offset of formations is interpreted to have occurred due to salt withdrawal in the source layer, whereas thinning of units at Hoodoo Dome is most apparent within formations that onlap salt wings or debris flows.

Subsurface deformation appears to be predominantly ductile at seismic scales (e.g. Fig. 8a); however, a few brittle faults are visible along the western margin of Dumbells Dome and adjacent to the eastern margin of Hoodoo Dome (as previously described in the previous section). Faulting on top of Hoodoo Dome is also present as indicated by previous regional mapping (Stott, 1969), but the presence of these faults is not resolved in seismic profiles due to low image quality in the top 500 ms of the data.

The most evident unconformities occur within the Isachsen Formation, cutting off draped and thinned Deer Bay and lower Isachsen deposits (Fig. 8c) and capping eroded Isachsen rim syncline deposits (Fig. 6). Unconformities are also visible within the Deer Bay Formation, accommodating much of the observed thinning (Figs 8d and 11b). The presence of salt wings and/or debris flows also suggests that there may be unconformities capping draped sediments (e.g. Jameson and McConnell formations, Fig. 8b–d) along Hoodoo Dome's margins.

BACKSTRIPPING ANALYSIS

The subsidence history of the Sverdrup Basin is recorded by its stratigraphy and can be separated using the backstripping method into subsidence related to isostatic effects due to loading of sediments and water and subsidence related to tectonic events (e.g. Steckler & Watts, 1978). Subsidence curves are generally produced by applying three corrections to present day compacted stratigraphic thicknesses: (1) decompaction, (2) paleobathymetry and (3) absolute sea level fluctuations or eustasy (Allen & Allen, 1990).

For this study, 1D backstripping was carried out with the Petroprob code (e.g. Van Wees & Beekman, 2000; Van Wees *et al.*, 2009) in an attempt to highlight possible regional tectonic triggers for diapirism, and to evaluate local subsidence variations in wells located adjacent to diapirs. The code adopts airy isostasy for basin loading with an assumed mantle density of $3400\ \mathrm{kg\ m^{-3}}$. Decompaction of units was completed using standard exponential porosity–depth curves (Van Wees *et al.*, 2009). Porosity–depth relationships are functions of the lithology, therefore the porosity of each unit is determined from the approximated percentages of each lithology (e.g. sandstone, siltstone, limestone, etc.).

Input parameters

Backstripping was carried out on a subset of 19 wells located on central and southern Ellef Ringnes Island and

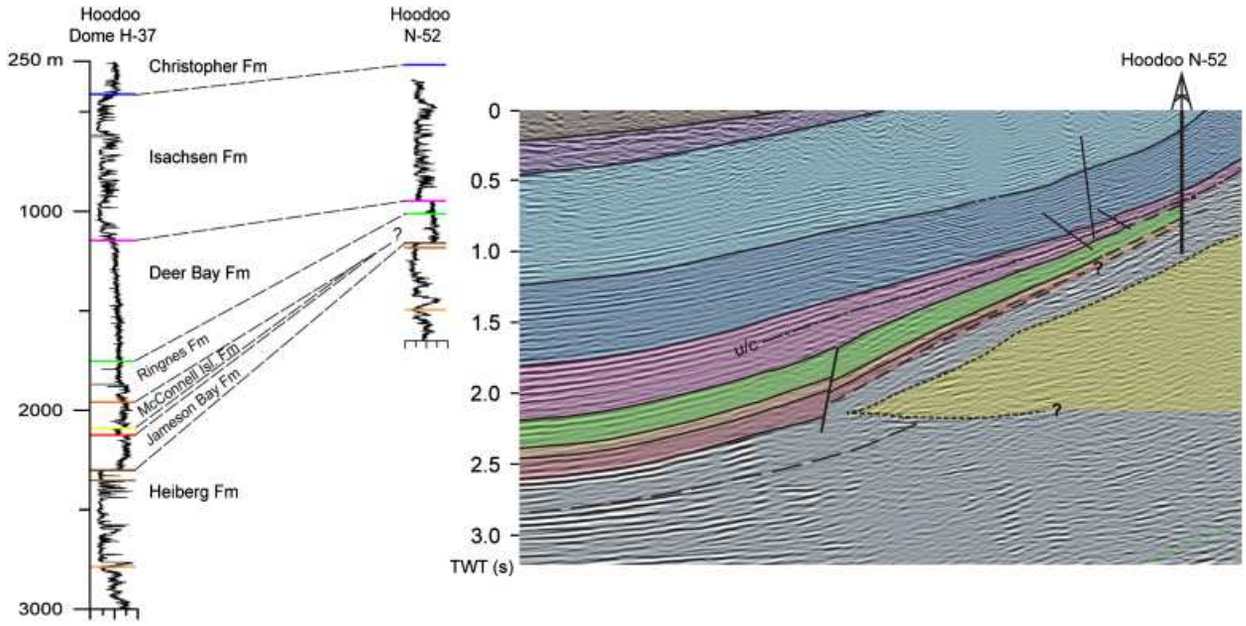

Fig. 11. Comparison of well logs for Hoodoo Dome H-37 and Hoodoo N-52, illustrating the decrease in formation thicknesses next to the Hoodoo Dome margin. Hoodoo N-52 well is overlain on a neighbouring seismic profile. The locations of Hoodoo N-52, Hoodoo Dome H-37 and the seismic profile are labelled on Fig. 2. The seismic profile is the property of Imperial Oil Resources.

King Christian Island (Fig. 2). All the chosen wells penetrate to at least the top of the Heiberg Formation or King Christian Formation. Stratigraphic time–depth pairs (thickness and age of formations) are based on reinterpreted formation tops from exploration wells (Dewing & Embry, 2007). This method differs from previous backstripping studies of the Sverdrup Basin (Stephenson *et al.*, 1987, 1994) where regional isopachs were used to determine basin-wide subsidence. The formation ages are estimated from stratigraphic columns produced for Ellef Ringnes Island by Dewing & Embry (2007). None of the wells intersect formations younger than Cenomanian age (e.g. Hassel, Kanguk and Expedition formations); therefore estimates of pre-erosion thicknesses were extrapolated from isochore maps (Fig. 9). Percentages of lithologies were estimated from borehole logs.

The results of this study are interpreted qualitatively in terms of general/regional tectonic events, and as such detailed local quantitative variations in depth-porosity-lithology are not of direct interest. Consequently, the effect of shallow paleobathymetry that existed from the Late Triassic (Norian) to Cretaceous is neglected as it does not alter general subsidence trends. In contrast, the effect of paleobathymetry before the Norian was substantial and cannot be neglected. Embry & Beauchamp (2008) suggest that the bathymetric difference between the basin margins and axis may have exceeded 2 km at the end of the Permian before being quickly filled during the Triassic. Unfortunately, the lack of sufficient constraints on the paleo water-depth during this time period does not permit us to implement this parameter properly. An attempt to include estimated water-depth parameters for the Early and Middle Triassic would lead only to higher frequency fluctuations in the curves, which may be a direct result of the large uncertainties of these approximations. The effects of errors in porosity–depth sampling, formation ages and paleobathymetry on tectonic and basin subsidence curves are included, by way of an example, for the Sutherland O-23 well in Fig. 12b.

Rates of subsidence within each formation are averaged due to age constraints, therefore rapid changes in basin subsidence restricted to shorter time periods may not be resolved. Errors in estimated formation thicknesses may also occur due to unidentified unconformities within wells. Erosion and unconformities are difficult to identify and approximate as contacts often appear conformable. Regional unconformities are frequent throughout the Mesozoic; however, the distribution of these unconformities is often restricted to the basin margins. Unconformities were therefore not included in the backstripping procedure as the estimation of erosion and timing of these unconformities would inherently contain errors. The exclusion of known unconformities in the backstripping procedure would lead to underestimation of periods of increased tectonic subsidence or sudden uplift. The effects of the exclusion of unconformities for various time periods are discussed in the section 'Evolution of piercement structures in the Mesozoic'.

Main results

Timing of tectonic events

Owing to the restriction of most well data to the Late Triassic, backstripping of wells is limited to 200 Ma. The total subsidence for a distinct period of basin evolution can be examined quantitatively; however, true tectonic subsidence rates and amounts require knowledge of the entire basin loading history and therefore general trends and

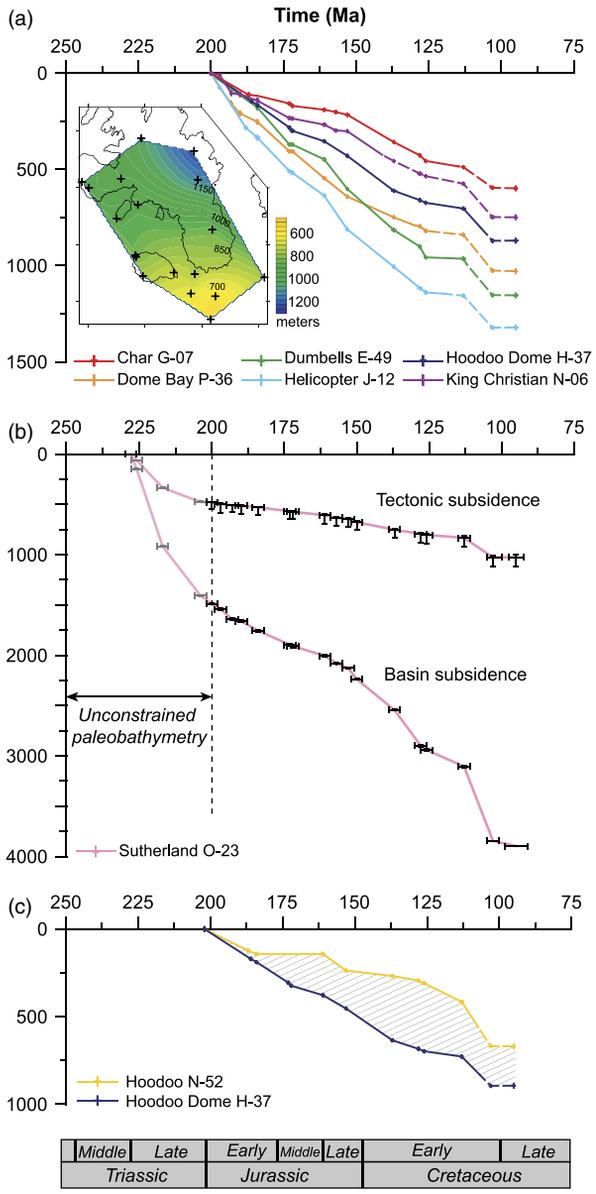

Fig. 12. (a) Tectonic subsidence of select wells dating to 200 Ma. The inset map includes contours of tectonic subsidence at 95 Ma. (b) Basin and tectonic subsidence profiles of Sutherland O-23 with error bars that include uncertainties in formation ages, decompaction and the effect of adding 100 m of paleobathymetry in the backstripping procedure. Paleobathymetry estimates were not taken into account for formations older than 200 Ma. (c) The local deviation of tectonic subsidence at Hoodoo N-52 due to the uplift of formations during diapirism is compared with regional tectonic curves (Hoodoo Dome H-37). The difference between the two curves is shaded in stippled grey. The locations of select wells are included in Fig. 2.

changes in tectonic subsidence rates for this study are only examined qualitatively.

Regionally, the majority of wells share similar trends in subsidence dating from 200 to 95 Ma (Fig. 12a). Relative rates of tectonic subsidence can be described generally in four stages: (1) The Rhaetian to Barremian (200–126 Ma) is considered to be a period of moderate tectonic subsidence with slight oscillations that vary among individual subsidence curves. Variations in the steady trend of these curves during this period are more common in wells located in the south (e.g. King Christian N-06 in Fig. 12a). (2) Subsidence patterns change in the Aptian during deposition of the Isachsen Formation from 126 to 113 Ma, recording a period of quiescence that is most pronounced in wells located further north in Noice Peninsula and further east toward Dumbells and Contour Dome (e.g. Dome Bay P-36 and Dumbells E-49). (3) The third stage in the Albian (113–103 Ma) records the highest rates of tectonic subsidence within the analyzed time period, followed by (4) a decrease in tectonic subsidence during the deposition of the Hassel Formation from 103 to 95 Ma.

Regional variation in tectonic subsidence

The similarity in the trends of tectonic subsidence (with the exception of Hoodoo N-52) suggests that tectonic influences were regional, however, the relative amounts of tectonic subsidence varies across Ellef Ringnes and King Christian Island. The regional trend in tectonic subsidence at 95 Ma is illustrated in the map inset of Fig. 12a for wells backstripped to 200 Ma. It should again be emphasized that these tectonic subsidence values are not quantitative as they do not include any effects of basin loading before 200 Ma, but instead show the relative distribution of tectonic subsidence between individual wells. The gradual trend toward higher subsidence rates in the east-central region of Ellef Ringnes Island is consistent throughout the Mesozoic and correlates with the progressive thickening of units from the south to northeast (Fig. 9).

Influence of diapirism on local subsidence curves

The distance of wells to the dome margins proved to be problematic in identifying local subsidence signatures related to salt movement. Hoodoo N-52 is the only well with a tectonic subsidence signature that significantly deviates from regional trends (Figs 11 and 12c) and provides the only constraint on the timing of diapir growth from subsidence curves. Hoodoo N-52 records a period of little to no tectonic subsidence from 185 to 126 Ma during which time average regional tectonic subsidence rates remain relatively steady. After 126 Ma, the deviation of Hoodoo N-52 from regional subsidence signatures (Hoodoo Dome H-37) decreases.

DISCUSSION

Triggering mechanisms of evaporite diapirism

Reactive diapirism, localization along basement faults, and differential loading from prograding sediments have been suggested to be possible triggering and initial localizing mechanisms of salt diapirs in the Sverdrup Basin (Gould & DeMille, 1964; Balkwill, 1978; Schwerdtner & Osadetz, 1983; Stephenson *et al.*, 1992; Jackson & Harrison,

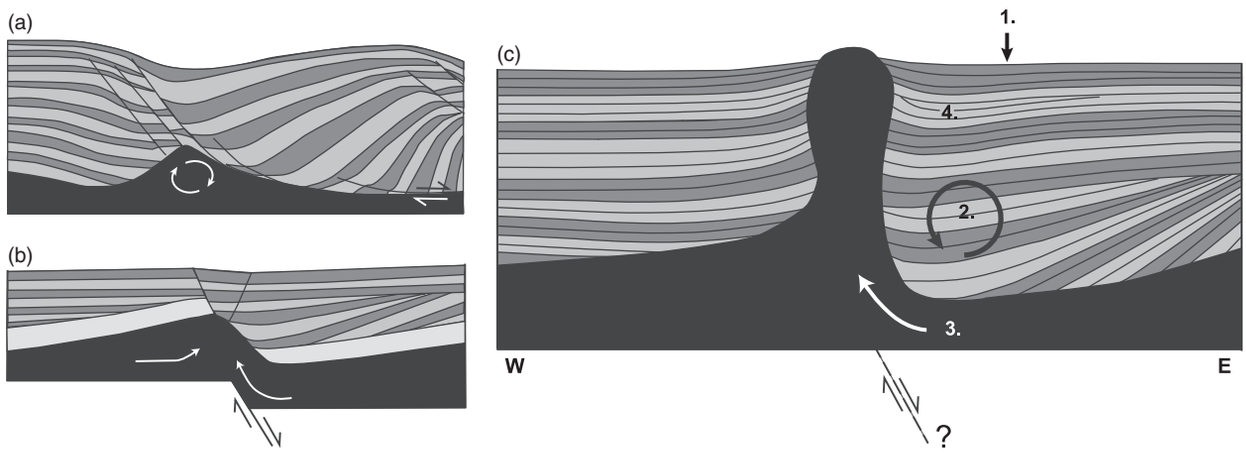

Fig. 13. First stages of diapir development controlled by faulting within (a) the overburden during thin-skinned extension and (b) the basement during thick-skinned extension (modified after Koyi *et al.* 1993a; Brun & Mauduit, 2009 respectively). (c) Schematic of a dome illustrating the positive feedback mechanism that drives excess sediment loading (1) and salt withdrawal (3) on an eastern downthrown fault graben. The feedback mechanism leads to the rotation of sedimentary beds (2), and formation of rim synclines (4) due to gravitational collapse.

2006). The linear to curvilinear outcrop patterns and asymmetric subsurface geometries of Hoodoo and Dumbells Domes, with thicker strata occurring at deeper structural levels along the east margin of the island, suggest that the localization and spatial distribution of these evaporite structures was most likely influenced by rift-related extensional faulting. These structures are thought to be north northwest–south southeast oriented normal faults (perpendicular to the basin axis) dipping to the east toward the Axel Heiberg depocentre (Fig. 1). The nature and timing of extensional faulting is not fully known as evidence for these structures is buried deep beneath the relatively conformable sedimentary basin fill. The formation of the diapirs could have been triggered by offset along basement faults, or by extensional faulting within the relatively thin cover during early periods of basin rifting. Thin-skinned and thick-skinned end-member scenarios and their expected characteristics are discussed below.

Thin-skinned extension

Vendeville & Jackson (1992a) highlighted the role of thin-skinned regional extension in initiating and promoting diapir growth (i.e. reactive diapirism). Regional extension forms normal faults in the brittle overburden, leading to the most effective avenue for evaporite piercement by weakening and thinning of the overlying sedimentary units. Salt rollers are low amplitude deflections at the upper surface of the salt layer that are generated below normal faults in overburden. More specifically, they are associated with tilted fault blocks and listric fault roll-over systems (overview in Brun & Mauduit, 2009). Fault growth/rollover systems are most often associated with passive margin settings (e.g. Gulf of Mexico) where evaporites or shale successions act as a decollement layer that allows the gravitational gliding and separation of overriding fault blocks along a tilted basement (e.g. Bally *et al.* 1981; Vendeville & Cobbold, 1987; Wu *et al.*, 1990; Cobbold & Szatmari, 1991; Ge *et al.*, 1997; Mauduit *et al.*, 1997; Mauduit & Brun, 1998).

In both tilted block and fault growth/rollover systems, the syn-sedimentary units form asymmetric profiles where the thickness of the formations increases with dip towards the fault (Fig. 13a). Rollover systems in particular produce fan-like syn-sedimentary layers that result from the interaction between a steeply dipping normal fault and an extending underlying ductile layer (Brun & Mauduit, 2008).

Balkwill (1978) suggested that salt may have originally been deposited on the Sverdrup Basin shelf and subsequently squeezed (coincident with gravitational gliding) toward the basin axis by thick prograding deposits originating from the southwest and from the eastern Ellesmere region. However, no seismic or stratigraphic data have yet been shown to support this. In addition, the evidence for such low amplitude structures is hard to preserve as their development and movement along basal surfaces varies throughout their evolution and they are buried deep below the sedimentary cover adjacent to diapir pedestals.

Thick-skinned extension

The concept of thick-skinned (i.e. basement involved) deformation as a trigger mechanism for diapirism during regional extension is in contrast to the widely accepted mechanism of thin-skinned deformation, or reactive diapirism (Vendeville & Jackson, 1992a, b). Jackson & Vendeville (1994) and Vendeville *et al.* (1995) argue that the effect of basement faults on salt diapirism is indirect unless salt is thin or depleted and that diapirism is more commonly triggered by thin-skinned extension. However, recurring observations of diapir asymmetry, lack of extensive overburden faulting and the spatial correlation of salt diapirs

to basement faults suggests that thick-skinned extension is also an important and common mechanism in triggering diapirism in many salt basins, such as the Dniepr-Donets Basin (Stovba & Stephenson, 2003), North Sea (Bishop, 1996), Danish Basin (Koyi & Petersen, 1993) and Nordkapp Basin (Koyi *et al*., 1993b). Numerical and analogue models have also confirmed the importance of basement geometry and structures induced by regional extension on the development of salt diapirs (e.g. Koyi, 1991; Koyi *et al*., 1993a; Nalpas & Brun, 1993; Withjack & Callaway, 2000).

Effective weakening of overburden within thick-skinned deformation settings occurs by the collapse of salt and overburden over basement faults (i.e. drape monoclines; e.g. Gaullier *et al*., 1993; Jackson & Vendeville, 1994; Withjack & Callaway, 2000), leading to forced folds and associated extension and fracturing within the overburden (Fig. 13b). The size and shape of the developing diapirs are governed by the localization of overburden deformation and salt flow, which is mainly controlled by a combination of the amount/rate of displacement along basement faults, the thickness of the salt and overburden, salt viscosity and the cohesive strength and ductility of the overburden (Koyi *et al*., 1993a; Nalpas & Brun, 1993; Withjack & Callaway, 2000). The rotation of basement blocks perturbs an unstable balance between salt and overburden, causing lateral variations in the thinning of both layers (Stovba & Stephenson, 2003).

The linear arrangement of diapirs in the Sverdrup Basin has been suggested previously as evidence for control by normal faults in the basement during the Mesozoic (Schwerdtner & Osadetz, 1983; van Berkel *et al*., 1983; Stephenson *et al*., 1992). Basement structures are expected in a rift basin but have not been resolved in previous gravity, seismic refraction or reflection studies conducted on Ellef Ringnes Island (e.g. Forsyth *et al*., 1979; Sobczak & Overton, 1984). More recent gravity modeling of the Canadian Arctic Innuitian region (Oakey & Stephenson, 2008) highlights several north–south trending linear features, one of which intersects Meteorologist Peninsula in southern Ellef Ringnes Island, just east of Hoodoo Dome and along strike with the Hoodoo anticline. However, the nature of this feature is unknown and it could be related to large-scale crustal deformation during the Eurekan Orogeny.

Driving mechanisms following diapir initiation

Once triggered by faulting, either in the subsurface and/or basin basement, linear salt structures may have continued to develop and mature into more discordant and higher amplitude salt stocks as the structures were continually modified by ongoing sedimentation. Their asymmetry would be perpetuated by differential loading during downbuilding (Talbot, 1977; Jackson & Talbot, 1986). Offset along basement faults or thin-skinned extensional faults displace overlying sediments (and evaporites in the case of thick-skinned deformation) on downthrown fault blocks by extensional collapse, creating accommodation space for thicker packages of sediments to accumulate. For the case of Ellef Ringnes Island, the differential loading of the proposed downthrown eastern fault blocks with respect to western fault blocks may have caused further subsidence into the underlying evaporite layer, which would further perpetuate loading of the fault block through a positive feedback mechanism (Fig. 13c). Owing to the positive feedback that drives increased subsidence along the eastern margin of the domes, the initial extensional fault is not required to slip continually during the history of dome growth. Differential loading would also result in the expulsion or withdrawal of salt beneath the downthrown fault blocks, effectively driving the growth of the neighbouring salt diapirs. Gravitational loading and withdrawal of salt along the eastern margins of the domes may have resulted in the following characteristics observed in seismic reflection profiles: thicker sedimentary units at deeper structural levels, development of more pronounced rim synclines, dramatic thinning of sediments at Dumbells Dome, diverging patterns of sedimentation at Hoodoo Dome, a near vertical shear zone adjacent to Hoodoo Dome, and more frequent occurrence of salt wings at Hoodoo Dome.

Evolution of piercement structures in the Mesozoic

Despite limitations in the quantitative analysis of tectonic subsidence, the primary focus of the study was to examine first-order subsidence signatures and relate them to observations from seismic profiles in terms of diapir growth. The general trends in subsidence rates are therefore sufficient to identify possible tectonic and sedimentary triggers that have affected and changed patterns of diapir growth. Diapir growth in relation to tectonism and sedimentary loading during the Mesozoic are subdivided into four stages below.

Early stages of diapirism in the Triassic

The diverging pattern of sedimentation toward the margin of Hoodoo Dome indicates that salt withdrawal beneath the overlying sedimentary units began as early as the Triassic, consistent with observations of deformed Triassic formations adjacent to other large domal diapirs located across the basin (e.g. Schwerdtner & Osadetz, 1983; van Berkel, 1989; Stephenson *et al*., 1992; Harrison, 1995). However, the timing of the event(s) that triggered the initial upward movement of salt is still unknown. Several tectonic events associated with faulting in the basement and/or basin sedimentary fill occurred in the Late Carboniferous to Early Triassic that may have triggered local perturbations in the Otto Fiord Formation and overlying sedimentary formations. From the Late Carboniferous to Early Permian, the basin experienced multiple pulses of tectonic quiescence separated by shorter intervals of uplift and fault-controlled differential subsidence (Embry & Beauchamp,

2008). This period is representative of a complex change in tectonic regime with orthogonal north–south rifting being replaced by transtension and transpression (Beauchamp *et al.*, 2001; Embry & Beauchamp, 2008).

These subtle tectonic events were followed by the 'Melvillian Disturbance' (Thorsteinsson & Tozer, 1970) in the Early-Middle Permian, responsible for a major base-level drop and folding and faulting of Upper Carboniferous and Permian strata (Thorsteinsson, 1974; Embry & Beauchamp, 2008). This event, primarily recorded in the southern margin of the basin (Thorsteinsson, 1974; Balkwill, 1978), is attributed to horst-and-graben tectonics where Melvillian folds are formed via draping over normal faulted blocks in the lower Palaeozoic basement (Harrison *et al.*, 1985, further discussion in Davies & Nassichuk, 1991).

Any one of these events may have triggered or accelerated diapir growth by thinning of overburden and pressurizing/localizing upward movement of evaporites. In future research, deeper penetration of the basin fill by higher resolution seismic reflection data and more age constraints on Middle Triassic and earlier sediments will be required to elucidate the age and nature of tectonic triggers of diapirism in the basin.

Passive diapirism in the Jurassic

The Jurassic and Early Cretaceous are marked by a period with a relatively steady rate of subsidence, which is interpreted by Stephenson *et al.* (1994) as a post-Palaeozoic rifting thermal subsidence phase. During this period, the style of deformation includes thinned and drape folded sedimentary units along diapir flanks. Thinned and drape folded units are often periodically truncated by unconformities, salt wings and/or debris flows. This suggests that sedimentation was greatly influenced by near surface salt rise in the Jurassic.

The formation of salt wings can occur via extrusion and burial of salt at the surface or by salt-wing intrusion along a weak stratigraphic horizon (such as evaporite) in the flanking sedimentary rock (Hudec & Jackson, 2006). There is no evidence that Mesozoic evaporite formations exist. Therefore, salt wing intrusion could only occur close to the surface, either along a buried extruded salt layer or along a weak unconsolidated shale layer. Subsidence trends from Hoodoo N-52 well also support ongoing diapir growth, suggesting that regional post-rift thermal subsidence at Hoodoo Dome margin was counteracted by salt growth to produce a time-averaged signature of tectonic quiescence for the majority of the Jurassic and Early Cretaceous (Fig. 12c).

Thinning and drape folding of the sedimentary flanks of rising diapirs are characteristic features of passive diapirism, such as the El Papalote diapir in northeastern Mexico (Giles & Lawton, 2002; Rowan *et al.*, 2003). Drape folding is produced by the rotation of near-surface strata along the uprising diapir flanks, and is accommodated by slip along bedding surfaces (Rowan *et al.*, 2003; Schultz-Ela, 2003). The unconformities and possible debris flows that truncate draped sediments along diapir flanks are also common features that form as the bathymetric scarp of the diapir becomes sufficiently steep that it fails gravitationally. Such mass transport facies produce the bounding surfaces of halokinetic sequences, or conformable strata influenced by near-surface salt rise (Giles & Lawton, 2002). The episodic nature of these sequences is caused by local rapidly fluctuating trends of sedimentation in relation to steady upward salt movement. These halokinetic sequences vary along the sides of the salt body and do not necessarily correlate with the regional dynamics of the basin (Giles & Lawton, 2002; Rowan *et al.*, 2003).

The formation of many of the features discussed above are generally considered characteristic of passive diapirism, however, they could also arise in compressional regimes (i.e. active diapirism; Rowan *et al.*, 2003). Characteristic features of active diapirism generally include thick arched roofs, narrow or pinched-off diapir stems, and include fold, thrusts, and or wrench blocks in adjacent strata (Dooley *et al.*, 2009 and references therein). Owing to the lack of seismic visibility at depth and within the diapir itself, only faulting and folding within adjacent sedimentary units could realistically be observed in this study. The lack of such features within the Jurassic sediments suggest that the predominant mechanism in the Jurassic to Early Cretaceous is passive diapirism where diapir growth is driven primarily by the response of overburden sinking into the source layer. Recent analogue experiments suggest, however, that diapir stocks can be squeezed in regional shortening without producing any deformation in adjacent strata, but this shortening must remain moderate (Dooley *et al.*, 2009). Regional tectonic subsidence curves and past basin studies (e.g. Embry, 1991; Embry & Beauchamp, 2008) do not identify any extended period of significant active regional compression. However, Stephenson *et al.* (1992) have suggested that moderate compression in the basin centre resulting from flexural bending of the syn-rift sediment layer due to sediment loading may have aided in accelerating diapir growth.

Diapirism and the effect of Amerasian Basin rifting in the Early Cretaceous

The onlap of the Hoodoo Dome salt wings, or the cessation in mass wasting events along the margins of the diapirs, by the Late Jurassic–Early Cretaceous formations (Deer Bay and Isachsen formations) marks a period of passive diapir growth where the aggradation rate (vertical accumulation of sediments) exceeded net diapiric rise (Talbot, 1995 and references therein). The increased aggradation rate corresponds to a period of increased sediment supply rate at the beginning of the Late Jurassic (Embry & Beauchamp, 2008), which is evidenced by total basin subsidence curves in the Ellef Ringnes Island region (Fig. 12b).

The Late Jurassic and Early Cretaceous period of aggradation and onlap was punctuated by several regional unconformities (late Valanginian–early Hauterivian,

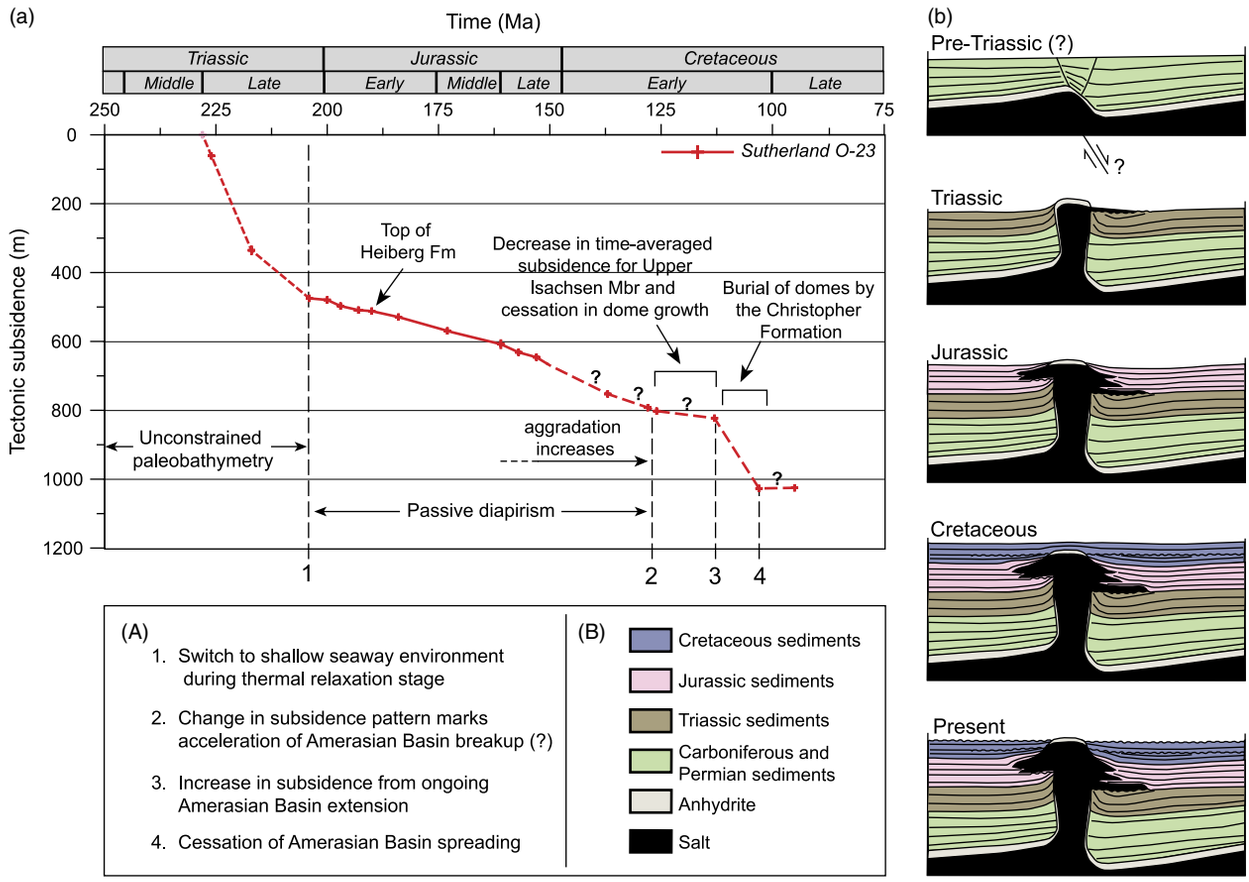

Fig. 14. (a) Interpreted tectonic phases and periods of diapirism superimposed on the Sutherland O-23 tectonic subsidence curve. Descriptions of tectonic phases are included in the key. Question marks along the subsidence curve mark the timing of regional unconformities identified by Embry & Beauchamp (2008). (b) Schematic diagrams illustrating the development of evaporite piercement structures (in particular Hoodoo Dome) on Ellef Ringnes Island.

mid-Barremian and mid-Aptian) during the deposition of the Isachsen Formation (Embry & Beauchamp, 2008). It is difficult to identify these unconformities and the corresponding amount of erosion on Ellef Ringnes Island seismic sections. To reduce further compounding errors due to estimates of the ages and amounts of erosion, the unconformities were not included in the backstripping procedure. As a result of our backstripping technique, rifting events may not be properly resolved in tectonic subsidence curves. For example, the largest of the unconformities, in the latest Valanginian–earliest Hauterivian, was interpreted by Embry & Dixon (1994) as widespread uplift related to the beginning of seafloor spreading and the creation of oceanic crust in the adjacent Amerasia Basin, known as the 'break-up unconformity'. This event is not resolved in our tectonic subsidence curves, where we observe instead ongoing subsidence with no change in tectonic subsidence rates. Only one seismic section (Fig. 8c) shows a clear unconformity flanking Hoodoo Dome near the base of the Isachsen Formation. However, on neighbouring Axel Heiberg Island the Hauterivian unconformity is well documented within flanking sedimentary units adjacent to several diapirs (Jackson & Harrison, 2006; Harrison & Jackson, 2008). During the Hauterivian hiatus, diapirs on Axel Heiberg Island shouldered aside their thin roofs, spread extrusively along the surface and coalesced to form a widespread canopy once subsequently buried (Jackson & Harrison, 2006). While the visualization of unconformities at Ellef Ringnes Island could be blamed by the low-resolution quality of the seismic data, it is still unclear why the style of salt structures varies between the Axel Heiberg WABS region and Ellef Ringnes Island. Many factors could be responsible, including variations in tectonic stress, sedimentary loading conditions, and the basement and salt-source layer architecture.

For this study, no noticeable change in regional tectonic subsidence curves are noted until 126–113 Ma (late Barremian to late Aptian), when a period of little to no tectonic subsidence is recorded. Because of the time averaged approach to examining regional tectonic subsidence, this period of no recorded tectonic subsidence could indicate uplift of the basin restricted to a much shorter time period(s) that was matched by continued subsidence occurring before or after an uplift event(s). Two other regional unconformities in the early Barremian and mid Aptian are common in the Sverdrup Basin (Embry & Beauchamp, 2008) and could account for the time averaged quiescence

observed during this period. The nicely defined unconformity that truncates rim syncline deposits east of Dumbells Dome (Fig. 6) is suspected to be related to one of these two regional unconformities. The unconformity at Dumbells Dome marks a significant change in the style of diapirism on Ellef Ringnes Island. Following this event, formations are less folded, vary less in thickness along the dome margins and continue to onlap or bury the domes completely. A change in the trend of Hoodoo N-52 tectonic subsidence also occurs at this time, with increased subsidence in relation to regional subsidence curves. This change suggests that the diapiric rise of Hoodoo Dome slowed during this period, perhaps allowing the onlap of the dome by Cretaceous formations.

The Aptian period of little to no tectonic subsidence observed in this study was followed by rapid tectonic subsidence and increased sedimentation during which the domes continued to be buried by the Christopher Formation from 113 to 103 Ma (Albian). The Albian event was previously recognized and attributed to a period of possible renewed extension, possibly indicating the initial rifting of the Amerasian Basin (Stephenson *et al.*, 1994). The uplift that occurred sometime between late Barremian and late Aptian, followed by rapid subsidence in the Albian are proposed to be both signatures that mark significant Amerasian Basin seafloor spreading events that dramatically altered the course of diapirism on Ellef Ringnes Island (Fig. 14). The Hauterivian (138–135 Ma) was previously interpreted as the most likely main rift onset or breakup unconformity based on the significant increase of normal fault activity and associated volcanism in the Sverdrup Basin following the unconformity (Embry & Dixon, 1994). However, recent ^{40}Ar–^{39}Ar dating of mafic magmatism in the Sverdrup Basin (Villeneuve & Williamson, 2006) suggests that the major pulse of igneous activity peaked later at 129–127 Ma. Hubbard *et al.* (1987) also commented on the significant influence of Amerasian rifting on stratigraphic/structural relationships in north Alaska and northwest Canada beginning at 128 Ma. The pulse of igneous activity, change in structural relationships in north Alaska and northwest Canada, and the change in subsidence patterns observed in this study suggest that Amerasian rifting activity may have amplified or accelerated around this time. Accelerated rifting of the Amerasian Basin north of Ellesmere Island may explain why the time-averaged Aptian signal is much stronger in tectonic subsidence curves located further north toward the Sverdrup Rim (e.g. Dumbells E-49 and Helicopter J-12). However, the strong tectonic signal observed in the northern most wells of this study could also be due to their location closer to the central axis of the basin.

Diapirism and the influence of the Eurekan Orogeny in the Late Cretaceous–Palaeogene

Tectonic subsidence data lacks the resolution to suggest that basin-wide tectonic events significantly influenced diapir growth in the Late Cretaceous once the domes were buried. The late Cenomanian unconformity near the Hassel Formation and Kanguk Formation boundary (Embry, 1991) correlates with an observed period of no long term tectonic subsidence dating between 103 and 95 Ma (e.g. Figs 12a or 14a). This suggests that the brief period of uplift in the late Cenomanian may have counteracted subsidence that occurred as the majority of Hassel Formation was being deposited. The unconformity may represent cessation of seafloor spreading in the Amerasia Basin (Embry & Dixon, 1994).

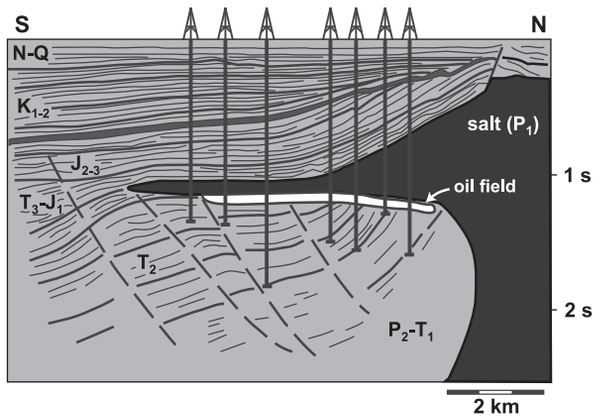

Fig. 15. An example of a canopy capping dipping sedimentary beds within the Pricaspian Basin (modified from Ismail-Zadeh *et al.* 2004). This particular canopy is found to cap an oil field whose spatial extent is confined from drilling. Similar circumstances may be present at Hoodoo Dome, or other diapirs within the Sverdrup Basin.

The Hassel Formation thins towards Hoodoo Dome (Gould & DeMille, 1964), suggesting that doming was still occurring during the Late Cretaceous, most likely driven by increased pressure in the source layer from continued downbuilding of adjacent sediments. Thicker deposits continued to accumulate on the east margin of Hoodoo Dome, possibly due to accommodation space that was continually provided by displacement on the shear zone along the eastern margin. The active piercement of overlying Cretaceous formations and exposure of the anhydrite caps at surface most likely occurred later due to the build-up of regional compression during the Eurekan orogeny. Although Ellef Ringnes Island is located away from the fold-and-thrust style of deformation that characterizes islands further to the east (Axel Heiberg and Ellesmere Island), weak evaporite diapirs most likely responded to mild shortening which led to the forced upward arching of adjacent strata and erosion along the flanks. The steep fault or shear zone on the eastern margin of Hoodoo Dome, parallel to the Hoodoo anticline, could also be a contractional kink band derived or reactivated by shortening in the diapir. Hoodoo Dome differs from Dumbells and Contour Dome as it does not fully pierce its sedimentary roof. One possible explanation is that the volume of salt fed into the diapir was partly distributed laterally to produce continued thickening of salt wings. The thickening of salt wings led to the upward deflection of sedimentary

horizons and produced unconformities within onlapping formations, as is seen in Fig. 11.

IMPLICATIONS FOR OIL AND GAS EXPLORATION

Petroleum exploration occurred in the Sverdrup Basin between 1969 and 1986, leading to the discovery of eight oil and 25 gas pools with estimated total proven reserves of 294×10^6 and $500 \times 10^9 m^3$, respectively (Chen *et al.*, 2000). Common traps offshore Ellef Ringnes Island include salt cored anticlines oriented orthogonal to the principle shortening direction of the Eurekan Orogeny. These high amplitude structures are under filled as a consequence of late growth in the Eocene and from possible fault/fracture leakage through extensive crestal faulting of the capping Jameson Bay Formation (Waylett & Embry, 1993). Owing to the low concentration of wells and seismic grid density, only large-scale features were detected during the 1969–1986 exploration programs. There is still significant potential for the discovery of higher frequency and more complex structures and traps with the advancement of imaging acquisition and processing techniques, in particular the ability to map the geometric complexity of traps with higher resolution 3D seismic surveys. Harrison (2001) suggests that new exploration plays could be developed in Carboniferous horst-and-graben settings, Permian inversion structures, Upper Palaeozoic unconformities, stratigraphic pinch-outs and in complex sub-salt structures.

Passive diapirs create the potential for many small oil and gas traps within surrounding deformed sediments (Stewart, 2006). Structural traps may include drape-folded and overturned sediments, unconformities, rim synclines, salt overhangs or wings and extensional radial and growth faults. For Hoodoo Dome in particular, salt wings and/or occurrence of stratal-flanking unconformities that truncate sandstone dominant formations such as the Heiberg Formation would make excellent traps and seals for oil and gas reservoirs. The impermeability of salt terminating and capping dragged sedimentary beds provides an excellent seal to oil and gas seepage (e.g. Fig. 15). The Heiberg Formation may also be locally truncated by impermeable shales of the Jameson Bay Formation by unconformities or debris flows that formed due to changes in the relative rates of sedimentation in relation to diapir movement. These traps would have developed in the Late Triassic to Early Jurassic, predating the main stage of petroleum generation and migration in the Cretaceous (Goodarzi *et al.*, 1989, 1993; Brooks *et al.*, 1992; Gentzis & Goodarzi, 1993).

CONCLUSIONS

This study highlights several distinct periods of salt diapir evolution on Ellef Ringnes Island throughout the Mesozoic, which are interpreted to be influenced by regional tectonic and sedimentary loading events. Major results and interpretations are summarized below:

(1) Hoodoo Dome and Dumbells Dome both exhibit asymmetric east–west profiles, with thicker accumulation of sediments at deeper structural levels east of the domes (Figs 6 and 7). The asymmetry matches the general trend in subsidence and sedimentary formation thicknesses directed towards the Axel Heiberg depocentre (Figs 9 and 12a, inset). The asymmetry is believed to be a product of the initial development of these structures along extensional faults within the overlying strata (thin-skinned extension) and/or above deep seated basement faults (thick-skinned extension). Asymmetric diapirs are believed to have continued evolving due to differential loading of sediments on adjacent fault blocks. The thick sedimentary fill in the basin centre prevents visualization of basement structures and architecture, diapir pedestals and prekinematic sedimentary layers, making it difficult to differentiate between the two possible trigger mechanisms.

(2) Diverging sedimentation and broad rim synclines suggest that diapirism began as early as the Early Triassic. The lack of resolution beyond the Triassic for both subsidence curves and seismic data limits further analysis of the diapirs' early evolution. Several tectonic events in the Late Carboniferous to Triassic, however, may be responsible for triggering diapirism by faulting and thinning within the sedimentary cover and/or faulting within the basement as suggested above.

(3) Jurassic formations flanking Hoodoo and Dumbells domes exhibit drape folded and thinned units. Hoodoo Dome also exhibits stratal cut-offs at the dome margins by local unconformities and salt wings and/or debris flows. Hoodoo N-52 well documents the thinning of units, and gives a tectonic subsidence signature that suggests that salt growth matched or exceeded regional post-rifting thermal subsidence during this period. Deformation of adjacent strata and backstripping analysis suggest that the diapirs were growing close to or at the surface in the Jurassic and are suspected to have evolved during a passive stage of growth. Active diapirism may have played a minor role in the development of the diapirs. However, insufficient evidence was found in this study to support this firmly.

(4) The aggradation rate increased at the beginning of the Early Cretaceous, leading to the onlap of salt wings and halokinetic sequences by the conformable Deer Bay and lower Isachsen members at Hoodoo Dome.

(5) A broad unconformity truncating rim syncline deposits on the eastern margin of Dumbells Dome marks a change in the general style of diapir development in the middle of the Early Cretaceous. Tectonic subsidence curves along Hoodoo Dome margin also suggest a decrease in diapir growth in relation to regional subsidence signatures on Ellef Ringnes Island. This rapid change in diapir development was followed by rapid

burial of the domes by the Christopher Formation, which terminated the growth of structures by passive diapirism. Regional uplift followed by rapid subsidence are thought to be signatures of accelerated rifting of the Amerasian Basin.

(6) Despite the burial of the domes by Early Cretaceous formations, the Hassel Formation continued to thin at dome margins during the Late Cretaceous, suggesting that doming was ongoing. The arched roofs and piercement of Cretaceous strata suggests that the diapirs forcefully uplifted and shouldered aside Cretaceous formations, most likely due to horizontal loading associated with the Eurekan Orogeny.

ACKNOWLEDGEMENTS

We thank K. Dewing (GSC) and C. Harrison (GSC) for their helpful insight on the project. J.D. Van Wees graciously provided us with the Petroprob code, used in our backstripping analysis. C. Schrank is thanked for help with the depth conversion of interpreted seismic horizons. Suncor Energy Inc., Imperial Oil Resources and PetroCanada kindly provided access to the legacy seismic and borehole data. Constructive reviews by A. Embry, M. Jackson, and M. Huuse greatly improved the clarity and accuracy of the manuscript. Funding to J.B. and A.C. included OGSST, NSERC Discovery and NRCan Unconventional Oil and Gas R&D grants. A.C. also thanks P. Budkewitsch (GSC) for the opportunity to carry out field work on Ellef Ringnes Island.

REFERENCES

Al-Chalabi, M. (1997) Time-depth relationships for multilayer depth conversion. *Geophys. Prospect.*, **45**, 715–720.

Allen, P.A. & Allen, J.R. (1990) *Basin Analysis: Principles and Applications*. Blackwell Scientific Publications, Oxford.

Balkwill, H.R. (1978) Evolution of Sverdrup Basin, Arctic Canada. *AAPG Bull.*, **62**, 1004–1028.

Balkwill, H.R. & Roy, K.J. (1978) King Christian Island, District of Franklin. Geological Survey of Canada, map 1445A.

Bally, A.W., Bernoulli, D., Davis, G.A. & Montadert, L. (1981) Listric normal fault. *Proceedings of the 26th International Geological Congress, Paris, 1980, Oceanol. Acta (SP)*, 87–101.

Beauchamp, B., Harrison, J.C., Utting, J., Brent, T.A. & Pinard, S. (2001) Carboniferous and Permian subsurface stratigraphy, Prince Patrick Island, Northwest Territories, Canadian Arctic. *Geol. Sur. Can. Bull.*, **565**, 93pp.

Bishop, D.J. (1996) Regional distribution and geometry of salt diapirs and supra-zechstein group faults in the Western and Central North Sea. *Mar. Petrol. Geol.*, **13**, 355–364.

Brooks, P.W., Embry, A.F., Goodarzi, F. & Stewart, R. (1992) Geochemical studies of Sverdrup Basin (Arctic Islands) – organic geochemistry and biological marker geochemistry of the Schei Point Group (Triassic) and recovered oils. *Bull. Can. Petrol. Geol.*, **40**, 173–187.

Brun, J.-P. & Mauduit, T.P.O. (2008) Rollovers in salt tectonics: the inadequacy of the listric fault model. *Tectonophysics*, **457**, 1–11.

Brun, J.-P. & Mauduit, T.P.O. (2009) Salt rollers: structure and kinematics from analogue modelling. *Mar. Petrol. Geol.*, **26**, 249–258.

Chen, Z., Osadetz, K.G., Embry, A.F., Gao, H. & Hannigan, P.K. (2000) Petroleum potential in western Sverdrup Basin, Canadian Arctic Archipelago. *Bull. Can. Petrol. Geol.*, **48**, 323–338.

Cobbold, P.R. & Szatmari, P. (1991) Radial gravitational gliding on passive margins. *Tectonophysics*, **188**, 249–289.

Davies, G.R. & Nassichuk, W.W. (1975) Subaqueous evaporites of the carboniferous Otto fiord formation, Canadian Arctic Archipelago: a summary. *Geology*, **3**, 273–278.

Davies, G.R. & Nassichuk, W.W. (1991) Carboniferous and Permian history of the Sverdrup Basin, Arctic Islands. In: *Geology of the Innuitian Orogen and Arctic Platform of Canada and Greenland*, (Ed. by H.P. Trettin) *Geol. Sur. Can.* **3**, 345–367.

Dewing, K. & Embry, A.F. (2007) Geological and geochemical data from the Canadian Arctic Islands. Part I: stratigraphic tops from Arctic Islands' oil and gas exploration boreholes. Geological Survey of Canada Open File, 5442

Dooley, T.P., Jackson, M.P.A. & Hudec, M.R. (2009) Inflation and deflation of deeply buried salt stocks during lateral shortening. *J. Struct. Geol.*, **31**, 582–600.

Embry, A. & Beauchamp, B. (2008) Sverdrup basin. In: *Sedimentary Basins of the World*, **Vol. 5** (Ed. by A. Miall), 451–471 Elsevier B.V., Amsterdam.

Embry, A.F. (1991) Mesozoic history of the Arctic Islands. Chapter 14. In: *Geology of the Innuitian Orogen and Arctic Platform of Canada and Greenland* Ed. by H.P. Trettin, *Geol. Sur. Can., Geol. Can.* **3**, 371–433.

Embry, A.F. & Dixon, J. (1994) *The Age of the Amerasia Basin*. 1992 Proceedings of the International Conference on Arctic Margins, Anchorage, U.S. Department of the Interior, Minerals Management Service.

Embry, A.F. & Osadetz, K.G. (1988) Stratigraphy and tectonic significance of cretaceous volcanism in the Queen Elizabeth Islands, Canadian Arctic Archipelago. *Can. J. Earth Sci.*, **25**, 1209–1219.

Forsyth, D.A., Mair, J.A. & Fraser, I. (1979) Crustal structure of the central Sverdrup Basin. *Can. J. Earth Sci.*, **16**, 1581–1598.

Fortier, Y.O., Blackadar, R.G., Glenister, B.F., Greiner, H.R., McLaren, D.J., McMillan, N.J., Norris, A.W., Roots, E.F., Souther, J.G., Thorsteinsson, R. & Tozer, E.T. (1963) Geology of the north-central part of the Arctic Archipelago, Northwest Territories (Operation Franklin). *Geol. Sur. Can. Mem.*, **320**, 671pp.

Gaullier, V., Brun, J.P., Guérin, G. & Lecanu, H. (1993) Raft tectonics: the effects of residual topography below a salt décollement. *Tectonophysics*, **228**, 363–381.

Ge, H., Jackson, M.P.A. & Vendeville, B.C. (1997) Kinematics and dynamics of salt tectonics driven by progradation. *AAPG Bull.*, **81**, 398–423.

Gentzis, T. & Goodarzi, F. (1993) Maturity studies and source-rock potential in the southern Sverdrup Basin, Arctic Canada. *Int. J. Coal Geol.*, **24**, 141–177.

Giles, K.A. & Lawton, T.F. (2002) Halokinetic sequence stratigraphy adjacent to the El Papalote Diapir, Northeastern Mexico. *AAPG Bull.*, **86**, 823–840.

Goodarzi, F., Brooks, P.W. & Embry, A.F. (1989) Regional maturity as determined by organic petrography and geochemistry of the Schei Point Group (Triassic) in the western Sverdrup Basin, Canadian Arctic Archipelago. *Mar. Petrol. Geol.*, **6**, 290–302.

Goodarzi, F., Gentzis, T., Embry, A.F., Osadetz, K.G., Skibo, D.N. & Stewart, K.R. (1993) Evaluation of maturity and source rock potential in the Lougheed Island Area of the central Sverdrup Basin, Arctic Canada. In: *Arctic Geology and Petroleum Potential* (Ed. by T.O. Vorren, E. Bergsager, O.A. Dahl-Stamnes, E. Holter, B. Johansen, E. Lie & T.B. Lund, *NPF Spec. Publ.* **2**, 147–157.

Gould, D.B. & Demille, G. (1964) Piercement structures in the Arctic Islands. *Bull. Can. Petrol. Geol.*, **12**, 719–753.

Harrison, J.C. (1995) Melville Island's salt-based fold belt, Arctic Canada. *Geol. Sur. Can. Bull.*, **472**, 1–1, 325pp.

Harrison, J.C. (2001) *Structural settings for hydrocarbon exploration in Canada's Arctic Islands*. Rock the Foundation Convention, CSPG Abstract, 5.

Harrison, J.C., Goodbody, Q.H. & Christie, R.L. (1985) Stratigraphic and structural studies on Melville Island, district of Franklin. *Curr. Res. A, Geol. Sur. Can. Pap.*, **85-1A**, 629–637.

Harrison, J.C. & Jackson, M.P.A. (2008) *Bedrock geology, strand fiord-expedition fiord area, Western Axel Heiberg Island, Northern Nunavut (Parts of Nts 59e, F, G and H)*. Geological Survey of Canada Open File, 5590

Heywood, W.W. (1955) Arctic piercement domes. *Can. Inst. Mining Metall.*, **58**, 27–32.

Hillis, R.R., Macklin, T.A. & Siffleet, P. (1995) Regional depth-conversion of mapped seismic two-way-times in the Cooper-Eromanga Basins. *Explor. Geophy.*, **26**, 412–418.

Hoen, E.W. (1964) *The anhydrite diapirs of central western Axel Heiberg Island*. Axel Heiberg Research Reports, McGill University. Montreal.

Hubbard, R.J., Edrich, S.P. & Peter Rattey, R. (1987) Geologic evolution and hydrocarbon habitat of the 'Arctic Alaska Microplate'. *Mar. Petrol. Geol.*, **4**, 2–35.

Hudec, M.R. & Jackson, M.P.A. (2006) Advance of allochthonous salt sheets in passive margins and orogens. *AAPG Bull.*, **90**, 1535–1564.

Hugon, H. & Schwerdtner, W.M. (1982) Discovery of halite in a small evaporite diapir on southeastern Axel Heiberg Island, Canadian Arctic Archipelago. *Bull. Can. Petrol. Geol.*, **30**, 303–305.

Ismail-Zadeh, A., Tsepelev, I., Talbot, C. & Korotkii, A. (2004) Three-dimensional forward and backward modelling of diapirism: numerical approach and its applicability to the evolution of salt structures in the Pricaspian Basin. *Tectonophysics*, **387**, 81–103.

Jackson, M.P.A. & Harrison, J.C. (2006) An allochthonous salt canopy on Axel Heiberg Island, Sverdrup Basin, Arctic Canada. *Geology*, **34**, 1045–1048.

Jackson, M.P.A. & Talbot, C.J. (1986) External shapes, strain rates, and dynamics of salt structures. *Geol. Soc. Am. Bull.*, **97**, 305–323.

Jackson, M.P.A. & Vendeville, B.C. (1994) Regional extension as a geologic trigger for diapirism. *Geol. Soc. Am. Bull.*, **106**, 57–73.

Koyi, H. (1991) Gravity overturns, extension, and basement fault activation. *J. Petrol. Geol.*, **14**, 117–142.

Koyi, H., Jenyon, M.K. & Petersen, K. (1993a) The effect of basement faulting on diapirism. *J. Petrol. Geol.*, **16**, 285–312.

Koyi, H. & Petersen, K. (1993) Influence of basement faults on the development of salt structures in the Danish Basin. *Mar. Petrol. Geol.*, **10**, 82–94.

Koyi, H., Talbot, C.J. & Tørudbakken, B.O. (1993b) Salt diapirs of the southwest Nordkapp Basin: analogue modelling. *Tectonophysics*, **228**, 167–187.

Larochelle, A. & Black, R.F. (1963) An application of paleomagnetism in estimating the age of rocks. *Nature*, **198**, 1260–1262.

Mauduit, T. & Brun, J.P. (1998) Growth fault/rollover systems: birth, growth, and decay. *J. Geophys. Res.*, **103**, 18119–18136.

Mauduit, T., Guerin, G., Brun, J.P. & Lecanu, H. (1997) Raft tectonics: the effects of basal slope angle and sedimentation rate on progressive extension. *J. Struct. Geol.*, **19**, 1219–1230.

Miall, A.D. (1984) Sedimentation and tectonics of a diffuse plate boundary: the Canadian Arctic Islands from 80 Ma B.P. to the present. *Tectonophysics*, **107**, 261–277.

Miall, A.D. (1991) Late Cretaceous and Tertiary basin development and sedimentation, Arctic Islands. Chapter 15. In: *Geology of the Innuitian Orogen and Arctic Platform of Canada and Greenland* (Ed. by H.P. Trettin, *Geol. Sur. Can., Geol. Can.* **3**, 437–458.

Nalpas, T. & Brun, J.P. (1993) Salt flow and diapirism related to extension at crustal scale. *Tectonophysics*, **228**, 349–362.

Oakey, G.N. & Stephenson, R. (2008) Crustal structure of the Innuitian region of Arctic Canada and Greenland from gravity modelling: implications for the Palaeogene Eurekan Orogen. *Geophys. J. Int.*, **173**, 1039–1063.

Ricketts, B.D. & Stephenson, R.A. (1994) The demise of Sverdrup Basin: late Cretaceous-Palaeogene sequence stratigraphy and forward modeling. *J. Sediment. Res. B: Stratigr. Global Stud.*, **64**, 516–530.

Rowan, M.G., Lawton, T.F., Giles, K.A. & Ratliff, R.A. (2003) Near-salt deformation in La Popa Basin, Mexico, and the Northern Gulf of Mexico: a general model for passive diapirism. *AAPG Bull.*, **87**, 733–756.

Schultz-Ela, D.D. (2003) Origin of drag folds bordering salt diapirs. *AAPG Bull.*, **87**, 757–780.

Schwerdtner, W.M. & Clark, A.R. (1967) Structural analysis of Mock Fiord and South Fiord Domes, Axel Hieberg Island, Canadian Arctic. *Can. J. Earth Sci.*, **4**, 1229–1245.

Schwerdtner, W.M. & Osadetz, K. (1983) Evaporite diapirism in the Sverdrup Basin (Canada): new insights and unsolved problems. *Bull. Can. Petrol. Geol.*, **31**, 27–36.

Sobczak, L.W. & Overton, A. (1984) Shallow and deep crustal structure of the western Sverdrup Basin, Arctic Canada. *Can. J. Earth Sci.*, **21**, 902–919.

Spector, A. & Hornal, R.W. (1970) Gravity studies over three evaporite piercement domes in the Canadian Arctic. *Geophysics*, **35**, 57–65.

Steckler, M.S. & Watts, A.B. (1978) Subsidence of the Atlantic-Type continental margin off New York. *Earth Planet. Sci. Lett.*, **41**, 1–13.

Stephenson, R., Boerstoel, J., Embry, A.F. & Ricketts, B.D. (1994) *Subsidence analysis and tectonic modelling of the Sverdrup Basin*. 1992 Proceedings, International Conference on Arctic Margins, Anchorage, U.S. Department of the Interior, Minerals Management Service.

Stephenson, R.A., Embry, A.F., Nakiboglu, S.M. & Hastaoglu, M.A. (1987) Rift-initiated permian to early cretaceous subsidence of the sverdrup basin. *Can. Soc. Petrol. Geol. Mem.*, **12**, 213–231.

Stephenson, R.A., Ricketts, B.D., Cloetingh, S.A. & Beekman, F. (1990) Lithosphere folds in the Eurekan Orogen, Arctic Canada? *Geology*, **18**, 603–606.

Stephenson, R.A., van Berkel, J.T. & Cloetingh, S.A.P.L. (1992) Relation between salt diapirism and the tectonic history of the Sverdrup Basin, Arctic Canada. *Can. J. Earth Sci.*, **29**, 2695–2705.

Stewart, S.A. (2006) Implications of passive salt diapir kinematics for reservoir segmentation by radial and concentric faults. *Mar. Petrol. Geol.*, **23**, 843–853.

Stott, D.F. (1969) Ellef Ringnes Island, Canadian Arctic Archipelago. *Geol. Sur. Can. Pap.*, **68-16**, 44pp.

Stovba, S.M. & Stephenson, R.A. (2003) Style and timing of salt tectonics in the Dniepr-Donets Basin (Ukraine): implications for triggering and driving mechanisms of salt movement in sedimentary basins. *Mar. Petrol. Geol.*, **19**, 1169–1189.

Talbot, C.J. (1977) Inclined and asymmetric upward-moving gravity structures. *Tectonophysics*, **42**, 159–181.

Talbot, C.J. (1995) Moulding of salt diapirs by stiff overburden. In: *Salt Tectonics: A Global Perspective for Exploration* (Ed. by M.P.A. Jackson, D.G. Roberts & S. Snelson, *AAPG Mem.* **65**, 61–75.

Thorsteinsson, R. (1974) Carboniferous and Permian stratigraphy of Axel Heiberg Island and western Ellesmere Island, Canadian Arctic Archipelago. *Geol. Sur. Can. Bull.*, **224**, 86pp.

Thorsteinsson, R. & Tozer, E.T. (1960) Summary account of structural history of the Canadian Arctic Archipelago since Precambrian time. *Geol. Sur. Can. Pap.*, **60-7**, 25pp.

Thorsteinsson, R. & Tozer, E.T. (1970) Geology of the Arctic Archipelago. *Geol. Econ. Miner. Can., Geol. Sur. Can.*, **1**, 547–591.

van Berkel, J.T. (1989) Deformation in the overburden of diapiric evaporite ridges: examples from the Sverdrup Basin, Canadian Arctic Archipelago. *J. Struct. Geol.*, **11**, 995–1006.

van Berkel, J.T., Hugon, H., Schwerdtner, W.M. & Bouchez, J.L. (1983) Study of anticlines, faults and diapirs in the central Eureka Sound Fold Belt, Canadian Arctic Islands: preliminary results. *Bull. Can. Petrol. Geol.*, **31**, 109–116.

van Berkel, J.T., Schwerdtner, W.M. & Torrance, J.G. (1984) Wall-and-Basin structure: an intriguing tectonic prototype in the central Sverdrup Basin, Canadian Arctic Archipelago. *Bull. Can. Petrol. Geol.*, **32**, 343–358.

Van Leeuwen, J. (2005) *Structure and mechanisms of emplacement of the Dumbells and Contour anhydrite domes, Ellef Ringnes Island, Canadian Arctic Archipelago*. Unpublished Bachelor's thesis, University of Toronto.

Van Wees, J.D. & Beekman, F. (2000) Lithosphere rheology during intraplate basin extension and inversion. Inferences from automated modeling of four basins in Western Europe. *Tectonophysics*, **320**, 219–242.

Van Wees, J.D., Van Bergen, F., David, P., Nepveu, M., Beekman, F., Cloetingh, S. & Bonté, D. (2009) Probabilistic tectonic heat flow modeling for basin maturation: assessment method and applications. *Mar. Petrol. Geol.*, **26**, 536–551.

Vendeville, B. & Cobbold, P.R. (1987) Glissements Gravitaires Synsedimentaires Et Failles Normales Listriques: modeles experimentaux. *C. R. Acad. Sci. Paris*, **305**, 1313–1319.

Vendeville, B.C., Ge, H. & Jackson, M.P.A. (1995) Scale models of salt tectonics during basement-involved extension. *Petrol. Geosci.*, **1**, 179–183.

Vendeville, B.C. & Jackson, M.P.A. (1992a) The rise of diapirs during thin-skinned extension. *Mar. Petrol. Geol.*, **9**, 331–354.

Vendeville, B.C. & Jackson, M.P.A. (1992b) The fall of diapirs during thin-skinned extension. *Mar. Petrol. Geol.*, **9**, 354–371.

Villeneuve, M. & Williamson, M.C. (2006) *^{40}Ar–^{39}Ar dating of mafic magmatism from the Sverdrup Basin Magmatic Province*. Proceedings of the Fourth International Conference on Arctic Margins, pp. 206–215.

Waylett, D.C. & Embry, A.F. (1993) Hydrocarbon loss from oil and gas fields of the Sverdrup Basin, Canadian Arctic Islands. In: *Arctic Geology and Petroleum Potential* (Ed. by T.O. Vorren, E. Bergsager, O.A. Dahl-Stamnes, E. Holter, B. Johansen, E. Lie & T.B. Lund, *NPF Spec. Publ.*, **2**, 195–204.

Withjack, M.O. & Callaway, S. (2000) Active normal faulting beneath a salt layer: an experimental study of deformation patterns in the cover sequence. *AAPG Bull.*, **84**, 627–651.

Wu, S., Bally, A.W. & Cramez, C. (1990) Allochthonous salt, structure and stratigraphy of the North-Eastern Gulf of Mexico. Part II: structure. *Mar. Petrol. Geol.*, **7**, 334–370.

